JEM Journal of Experimental Medicine

ARTICLE

The histone demethylase Lsd1 regulates multiple repressive gene programs during T cell development

Daniel B. Stamos[1*], Lauren M. Clubb[1*], Apratim Mitra[2], Laura B. Chopp[3], Jia Nie[3], Yi Ding[4], Arundhoti Das[4], Harini Venkataganesh[1], Jan Lee[1], Dalal El-Khoury[1], LiQi Li[1], Avinash Bhandoola[4], Remy Bosselut[3], and Paul E. Love[1]

Analysis of the transcriptional profiles of developing thymocytes has shown that T lineage commitment is associated with loss of stem cell and early progenitor gene signatures and the acquisition of T cell gene signatures. Less well understood are the epigenetic alterations that accompany or enable these transcriptional changes. Here, we show that the histone demethylase Lsd1 (Kdm1a) performs a key role in extinguishing stem/progenitor transcriptional programs in addition to key repressive gene programs during thymocyte maturation. Deletion of *Lsd1* caused a block in late T cell development and resulted in overexpression of interferon response genes as well as genes regulated by the Gfi1, Bcl6, and, most prominently, Bcl11b transcriptional repressors in CD4$^+$CD8$^+$ thymocytes. Transcriptional overexpression in *Lsd1*-deficient thymocytes was not always associated with increased H3K4 trimethylation at gene promoters, indicating that Lsd1 indirectly affects the expression of many genes. Together, these results identify a critical function for Lsd1 in the epigenetic regulation of multiple repressive gene signatures during T cell development.

Introduction

A hallmark of early T cell development is the down-regulation of hematopoietic stem cell (HSC) signature genes and the loss of alternative lineage potentials as double-negative (DN) thymocytes respond to maturational cues that promote commitment to the T lineage (Rothenberg et al., 2016). CD4$^-$CD8$^-$ DN stage 1 thymocytes (DN1; also referred to as early T progenitors [ETPs]) closely resemble, both phenotypically and transcriptionally, multipotent HSCs/progenitor cells (Zhang et al., 2012). With the exception of the erythroid/megakaryocyte lineage, DN1/DN2 cells retain the potential to commit to and develop into all hematopoietic lineages, including myeloid cells, innate immune cells (innate lymphoid cells [ILCs] and natural killer [NK] cells), and B lymphocytes (Shah and Zúñiga-Pflücker, 2014). In vitro differentiation experiments have established that commitment to the T lineage occurs between the DN2 and DN3 stages with commitment to the αβ or γδ T lineage taking place in DN3 cells (Ciofani and Zúñiga-Pflücker, 2010; Hayes and Love, 2007; Yui et al., 2010).

Considerable insight into the transcriptional program of developing thymocytes has been gained by microarray analysis or deep sequencing (RNA sequencing [RNA-seq]) of expressed mRNAs at each stage from ETP-DN1 through the mature CD4 single-positive (SP) or CD8 SP stage (Mingueneau et al., 2013; Zhang et al., 2012). These studies have shown that T lineage commitment is associated with the termination of HSC signature genes followed by the induction of DN stage-specific genes and ultimately the induction of T lineage–specifying genes (e.g., *Tcf7*, *Bcl11b*, *Gata3*, and *Runx3*). Less well understood are the epigenetic changes (DNA methylation and histone acetylation and/or methylation) that accompany and presumably enforce T lineage commitment and thymocyte maturation by regulating gene transcription. Given the striking shift from HSC/progenitor gene expression to T lineage gene expression that accompanies early DN development, much attention has focused on epigenetic mechanisms of gene silencing. In particular, the deposition of repressive trimethylated H3K27 marks (H3K27me3) at the promoters and known regulatory elements of HSC genes was recently investigated in several studies (Li et al., 2014; Manna et al., 2015; Mingueneau et al., 2013; Tanaka et al., 2013). Unexpectedly, the results of these studies revealed that while correlating with gene silencing, H3K27me3 decoration is not a widespread mechanism for HSC gene repression, nor does it

[1]Section on Hematopoiesis and Lymphocyte Biology, Eunice Kennedy Shriver National Institute of Child Health and Human Development, National Institutes of Health, Bethesda, MD; [2]Bioinformatics and Scientific Programing Core, Eunice Kennedy Shriver National Institute of Child Health and Human Development, National Institutes of Health, Bethesda, MD; [3]Laboratory of Immune Cell Biology, Center for Cancer Research, National Cancer Institute, Bethesda, MD; [4]Laboratory of Genome Integrity, Center for Cancer Research, National Cancer Institute, Bethesda, MD.

*D.B. Stamos and L.M. Clubb contributed equally to this paper; Correspondence to Paul E. Love: lovep@mail.nih.gov.

appear to be a consistently durable method of gene silencing (Manna et al., 2015; Zhang et al., 2012). It was recently demonstrated that the effects of loss of the H3K27 demethylases Jmjd3 and Utx on gene expression during CD4$^+$CD8$^+$ (double positive [DP]) to SP T cell development, while significant, were restricted to a surprisingly small number of genes that function at late stages of T cell maturation (Manna et al., 2015).

A second epigenetic mechanism for gene silencing is the removal of activating histone modifications, especially promoter-associated H3K4 methylation. The histone-3 Lysine (K)-4 demethylase Kdm1a (hereafter referred to as Lsd1), which removes di- or monomethylated H3K4 marks (H3K4me1, H3K4me2), can function as the catalytic subunit of CoREST (corepressor for element-1-silencing transcription factor) or NuRD (nucleosome remodeling and histone deacetylation) repressor complexes (Hosseini and Minucci, 2017). Notably, inhibition of Lsd1 activity in embryonic stem cells prevents their differentiation and the down-regulation of pluripotent genes (Whyte et al., 2012). In addition, it was recently shown that deletion of *Lsd1* in HSCs is associated with reduced H3K4me3 but increased H3K4me1 and H3K4me2 decoration at HSC gene promoters and failure to repress HSC genes during myelopoiesis (Kerenyi et al., 2013).

In the present study, we investigated the role of Lsd1 in T cell development by deletion of *Lsd1* specifically in immature DN thymocytes. Deletion of *Lsd1* resulted in a reduction in DP and CD4 SP thymocytes and defective DP-SP thymocyte maturation. Early HSC and DN stage-specific genes, including *Ctla4* and *Prdm1*, failed to be down-regulated, and several signature myeloid, innate lymphoid, and B cell genes failed to be repressed in *Lsd1*-deficient DP thymocytes, although loss of Lsd1 did not result in lineage divergence. Notably, targets of Lsd1-dependent Gfi1, Bcl6, or Bcl11b repressive complexes were overexpressed in Lsd1-deficient thymocytes and T cells. Most prominently, alterations in gene expression in Lsd1-deficient DP thymocytes, and the developmental consequences of these transcriptional changes, phenocopied those produced by deletion of the transcription factor Bcl11b, establishing an important role for Lsd1 in Bcl11b-mediated transcriptional repression. Altered gene expression was frequently but not always associated with enhanced H3K4me3 decoration at the promoters of mis-/overexpressed genes, indicating that Lsd1 mainly controls expression of a core group of key regulatory genes. Together, these results establish Lsd1 as a critical factor for multiple repressive transcriptional programs during T cell development.

Results

Deletion of Lsd1 in immature DN thymocytes inhibits thymocyte development

To assess the role of Lsd1 in T cell development, we generated *CD2-iCre;Lsd1$^{fl/fl}$* mice to extinguish expression of Lsd1 specifically in immature DN thymocytes. Intracellular staining of WT (Cre-negative *Lsd1$^{fl/fl}$*) thymocytes demonstrated that Lsd1 is expressed at all stages (DN1–4) of DN maturation and in DP and SP thymocytes (Fig. 1 A). In thymocytes from *CD2-iCre;Lsd1$^{fl/fl}$* mice, a reduction in Lsd1 protein was first observed at the DN3 stage (Fig. 1 A). Lsd1 expression was not detected in DP, CD4 SP, and CD8 SP thymocytes or in CD4$^+$ and CD8$^+$ peripheral T cells from *CD2-iCre;Lsd1$^{fl/fl}$* mice (Fig. 1 A and data not shown). Thus, in *CD2-iCre;Lsd1$^{fl/fl}$* mice, Lsd1 expression was significantly reduced in late-stage DN (DN3/4) thymocytes and was absent at the DP stage and thereafter.

The number of DN thymocytes was reduced in *CD2-iCre;Lsd1$^{fl/fl}$* mice (Fig. 1 B); however, no defects in the DN1–4 stages were evident, suggesting that there was no stage-specific block in DN maturation (Fig. S1 A). DP and CD4 SP but not CD8 SP thymocytes were markedly reduced in *CD2-iCre;Lsd1$^{fl/fl}$* mice (Fig. 1, B and C). The percentage and the number of mature TCR^{hi} CD24^{lo} CD4 SP and CD8 SP thymocytes were reduced in 2-wk-old *CD2-iCre;Lsd1$^{fl/fl}$* mice, indicating that late-stage development of SP cells was impaired in the absence of Lsd1 (Fig. 1 D and data not shown). Also, TCR^{lo} CD24^{hi} (immature SP [ISP]) CD8 thymocytes were increased in *CD2-iCre;Lsd1$^{fl/fl}$* mice, accounting for the normal number of total CD8 thymocytes (Fig. 1, B and D; and data not shown).

CD2-iCre;Lsd1$^{fl/fl}$ mice were lymphopenic due to a reduction in both CD4$^+$ and CD8$^+$ T cells (Fig. 2, A and B). A higher percentage of peripheral T cells from these mice were CD44^{hi} CD62L^{low} (Fig. 2 C), with the "memory-like" phenotype presumably reflecting lymphopenia-induced expansion (Voehringer et al., 2008). In contrast to younger mice, the percentage of mature TCR^{hi} CD24^{lo} CD4 SP and CD8 SP thymocytes was increased in adult (>8 wk old) *CD2-iCre;Lsd1$^{fl/fl}$* mice, although these mice remained lymphopenic, suggesting a defect in thymocyte emigration (Fig. 2 D). Consistent with this interpretation, expression of S1pr1, which is required for thymocyte emigration, was reduced on mature SP thymocytes from *CD2-iCre;Lsd1$^{fl/fl}$* mice (Fig. 2 E).

CD2-iCre;Lsd1$^{fl/fl}$ mice contained increased percentages of FoxP3$^+$ CD4$^+$ T regulatory (Treg) cells that were confirmed to be Lsd1 deficient (Fig. S1 B) and also contained increased numbers and percentages of DN γδTCR$^+$ thymocytes and T cells (Fig. 2 F and data not shown). To verify that the phenotype observed in *CD2-iCre;Lsd1$^{fl/fl}$* mice was due entirely to loss of Lsd1 and not to potential secondary effects of the Cre transgene, we generated *Rag1-Cre;Lsd1$^{fl/fl}$* mice. The kinetics of *Rag1* promoter–driven Cre activity was similar to that observed in *CD2-iCre;Lsd1$^{fl/fl}$* mice as assessed by Lsd1 intracellular staining, and the phenotype of *Rag1-Cre;Lsd1$^{fl/fl}$* mice closely resembled that of *CD2-iCre;Lsd1$^{fl/fl}$* mice, including the DN-DP developmental block, the block in CD4 SP and CD8 SP thymocyte maturation, and an increase in the percentage of Treg cells and γδTCR$^+$ thymocytes (data not shown). We also generated bone marrow chimeras by reconstituting lethally irradiated B6:CD45.1 mice with a 1:1 mixture of lineage-depleted bone marrow from B6 (CD45.1/2) mice and *CD2-iCre;Lsd1$^{fl/fl}$* (CD45.2) mice. The phenotype of *CD2-iCre;Lsd1$^{fl/fl}$* thymocytes derived from the bone marrow chimeras was similar to that of donor *CD2-iCre;Lsd1$^{fl/fl}$* mice in all respects (specifically, a more severe developmental block was not observed), indicating that the defects caused by *Lsd1* deletion were not exacerbated under competitive conditions (data not shown). To determine if the late-stage developmental defects observed in *CD2-iCre;Lsd1$^{fl/fl}$* thymocytes reflected a specific requirement for Lsd1 at this point or resulted from earlier effects of Lsd1

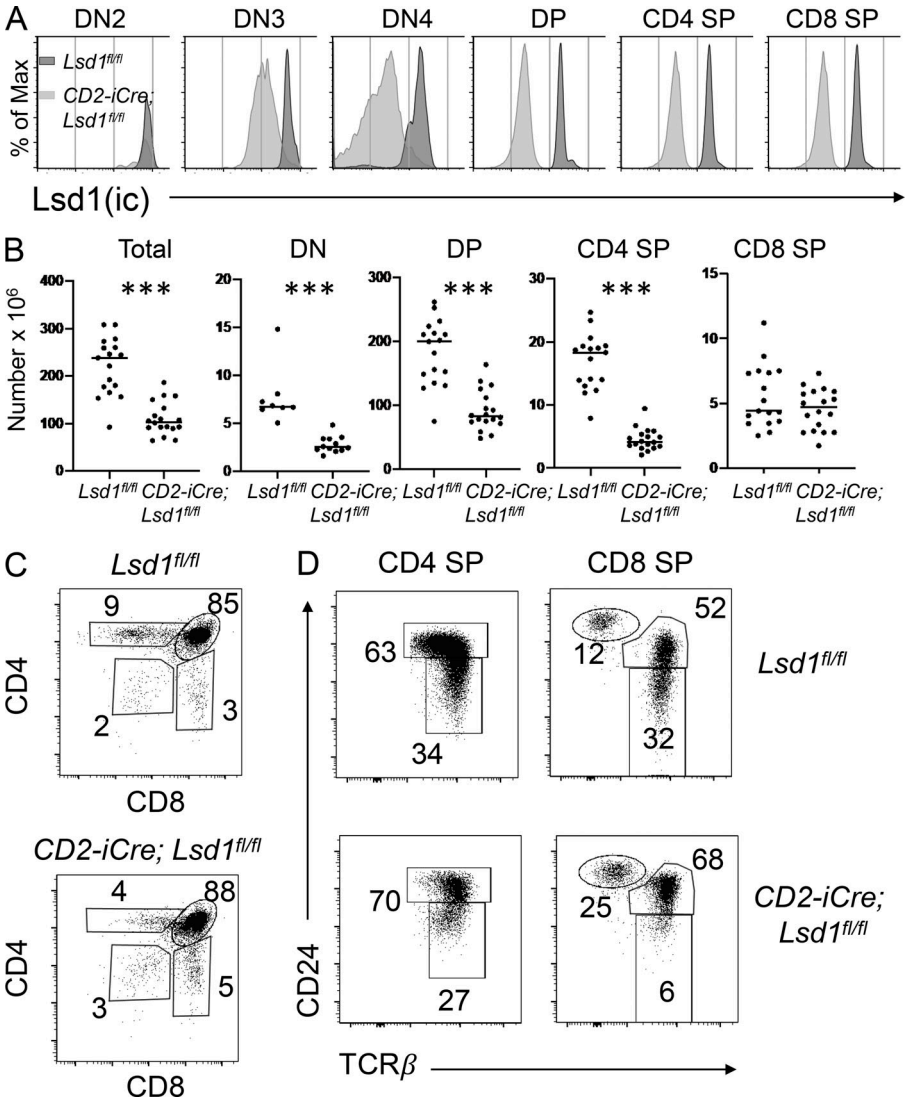

Figure 1. **Deletion of *Lsd1* causes a block in late T cell development. (A)** Intracellular staining of gated thymocyte subsets from control, *Lsd1*$^{fl/fl}$, and *CD2-iCre;Lsd1*$^{fl/fl}$ mice for Lsd1 protein. **(B)** Counts of the indicated thymocyte subsets from adult 4–8-wk-old *Lsd1*$^{fl/fl}$ and *CD2-iCre;Lsd1*$^{fl/fl}$ mice. ***, P < 0.005; unpaired *t* test. **(C)** Representative CD4 versus CD8 surface staining profile of total thymocytes from 2-wk-old *Lsd1*$^{fl/fl}$ and *CD2-iCre;Lsd1*$^{fl/fl}$ mice. Numbers are percentages of total cells in each gate. **(D)** CD24 versus TCRβ staining profiles of gated CD4 SP and CD8 SP thymocytes from 2-wk-old mice showing a maturational defect in thymocytes from *CD2-iCre;Lsd1*$^{fl/fl}$ mice. Results shown in A, C, and D are representative of three or more experiments.

deficiency, we also generated *CD4-Cre;Lsd1*$^{fl/fl}$ mice in which deletion of *Lsd1* begins at the DP stage and is complete by the SP stage (Fig. S1 C). T cell development appeared unaffected in *CD4-Cre;Lsd1*$^{fl/fl}$ mice (Fig. S1 D) that contained normal numbers of DP and SP thymocytes and peripheral T cells (Fig. S1 E and data not shown). Together, these results identified a critical function for Lsd1 in T cell development specifically at the DN–DP transition.

A limited functional survey revealed that *CD2-iCre;Lsd1*$^{fl/fl}$ T cells could be activated (based on TCR- induced CD69 up-regulation) and could proliferate and produce cytokines (IFNγ) and effector molecules (granzyme B) in response to TCR or TCR + CD28 costimulation; however, the latter responses were moderately impaired relative to those in *Lsd1*$^{fl/fl}$ control T cells (data not shown).

Deletion of *Lsd1* results in marked gene up-regulation in DP thymocytes

To examine the effect of *Lsd1* deletion at the transcriptional level, we performed deep sequencing of mRNAs (RNA-seq) from sorted DP thymocytes. We analyzed two subsets of DP cells from control WT (*Lsd1*$^{fl/fl}$) and KO (*CD2-iCre;Lsd1*$^{fl/fl}$) mice: TCR^{lo} CD69^{-} DP cells, which are the most immature post-ISP DP thymocyte subset, and TCR^{lo} CD69^{+} DP cells, which are composed of thymocytes that have received TCR selection signals and represent the next step of development after the CD69^{-} stage (Fig. 3 A). Principal component analysis (PCA) revealed considerable variance in the corresponding WT and KO DP subsets (Fig. 3 B; PC1, 54%). Using a cutoff of false discovery rate (FDR) <0.05, $|(\log_2$ fold change [$\log_2$FC])$|$ ≥1 yielded 3,676 dysregulated genes in the CD69^{-} and 3,105 dysregulated genes in the CD69^{+} WT versus KO comparisons, respectively (Fig. 3 C). Notably, the majority of dysregulated genes in KO thymocytes were up-regulated in both the KO versus WT DP CD69^{-} comparison (3,185 of 3,676 [87%]) and the KO versus WT DP CD69^{+} comparison (2,227 of 3,105 [72%]), consistent with a predominantly inhibitory role for Lsd1 in regulating gene expression (Fig. 3, C and D). (Note: "Up-regulated" or "overexpressed" in this case refers to gene expression in KO versus WT DP thymocytes and does not imply increased expression in DP cells relative to DN cells. In most instances, deletion of *Lsd1* resulted in continued expression of genes that are normally down-regulated at the DN to DP

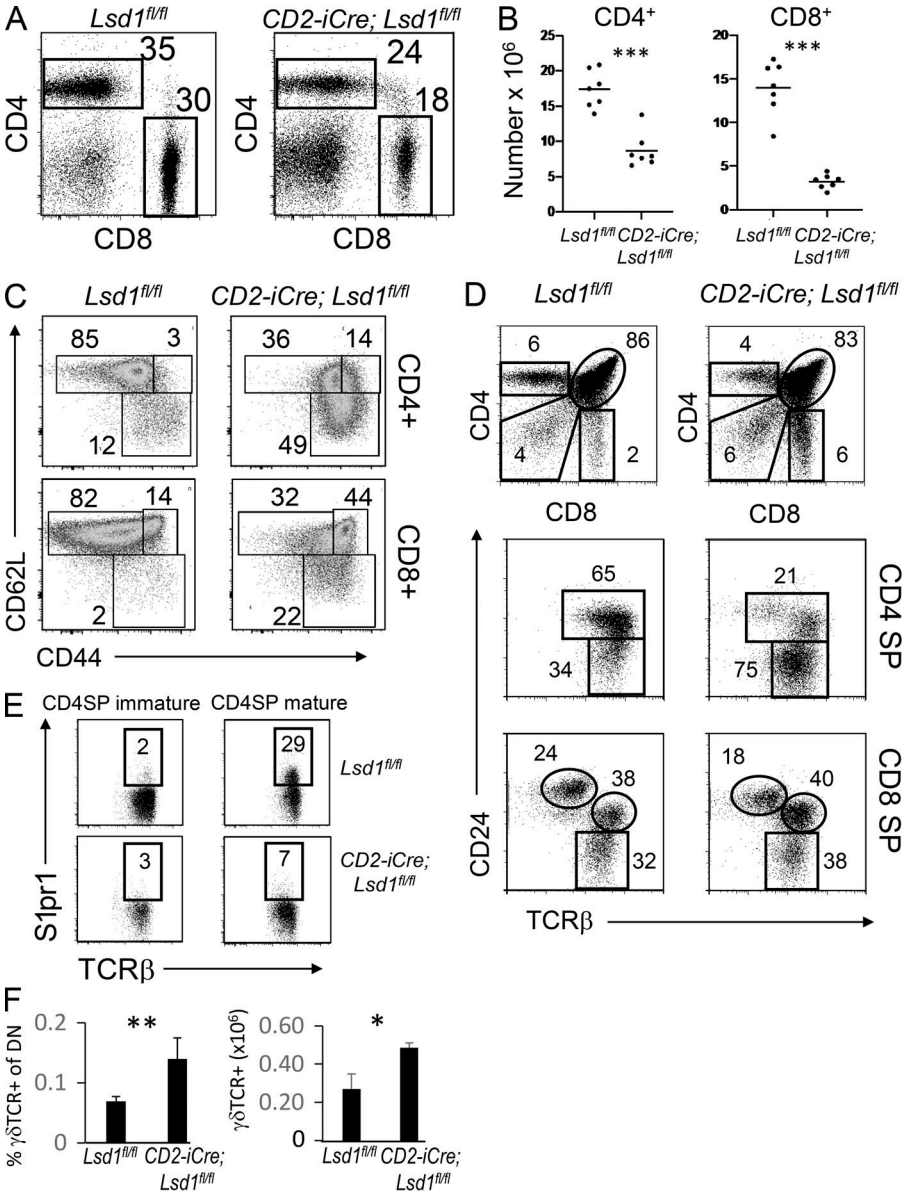

Figure 2. **A thymocyte emigration defect in adult *CD2-iCre;Lsd1$^{fl/fl}$* mice. (A)** CD4 versus CD8 surface staining profiles of total LN cells from 8-wk-old *Lsd1$^{fl/fl}$* and *CD2-iCre;Lsd1$^{fl/fl}$* mice. Numbers in each gate are the percentages of total cells. **(B)** Number of LN CD4$^+$ and CD8$^+$ T cells in 8-wk-old *Lsd1$^{fl/fl}$* and *CD2-iCre;Lsd1$^{fl/fl}$* mice. **(C)** CD62L versus CD44 surface staining of gated CD4$^+$ or CD8$^+$ T cells from *Lsd1$^{fl/fl}$* and *CD2-iCre;Lsd1$^{fl/fl}$* mice showing CD44^{hi} "memory-like" phenotype of T cells in *CD2-iCre;Lsd1$^{fl/fl}$* mice. **(D)** Phenotype of thymocytes from adult *Lsd1$^{fl/fl}$* and *CD2-iCre;Lsd1$^{fl/fl}$* mice. Numbers in each gate are percentages of total cells. **(E)** Staining of immature CD4$^+$CD24^{hi} and mature CD4$^+$CD24^{lo} thymocytes for S1pr1. **(F)** Percentage and number of γδTCR$^+$ thymocytes in adult *Lsd1$^{fl/fl}$* and *CD2-iCre;Lsd1$^{fl/fl}$* mice. *, P < 0.05; **, P < 0.01; ***, P < 0.005; unpaired *t* test. Data are represented as mean ± SEM. Results shown in A–E are representative of three or more experiments.

transition in DP thymocytes at levels similar to those in DN thymocytes.)

Two results suggested that *Lsd1* deletion had a greater impact on gene expression at the DN to DP transition stage than the DP CD69$^-$ to DP CD69$^+$ transition stage. First, the DP CD69$^-$ to DP CD69$^+$ transition stage accounted for a smaller proportion of variance in the gene expression data than the effect of the Lsd1-KO at either stage, as shown by Fig. 3 B. Second, most of the overexpressed genes (1,629 of 2,227 [73%]) in KO DP CD69$^+$ thymocytes were already overexpressed at the CD69$^-$ stage (Fig. S2, A and B). Together, these findings identified an important role for Lsd1 in the down-regulation of numerous genes during the DN to DP transition stage.

Functional enrichment analysis (gene ontology biological process) indicated that the overexpressed genes in *Lsd1* KO DP thymocytes (both CD69$^-$ and CD69$^+$) were predominantly involved in hematopoietic/immune system and innate immune/IFN/viral response–related functions, whereas down-regulated genes (which were much fewer in number) had functions predominantly related to chromatin assembly/segregation and cell division (Fig. 3 E and data not shown). A possible explanation for the latter finding is that an increased fraction of *Lsd1* KO thymocytes were quiescent (G_0 phase; Fig. S2 C), and expression of *Cdk6* and *cyclin D3*, which regulate the transition from G_0 to G_1 phase (Wells and Morawski, 2014), were down-regulated in KO DP thymocytes (Fig. S2 D). The increased expression of viral response and IFN response genes in *Lsd1* KO DP thymocytes (Fig. S3 A) was consistent with a previous report demonstrating that inhibition or knockdown of Lsd1 in adult mice results in endogenous retrovirus induction and down-regulation of the RNA-induced silencing complex, resulting in activation of the double-stranded RNA-IFN pathway in tumor cells, and suggests that *Lsd1* ablation in thymocytes results in a similar response (Sheng et al., 2018).

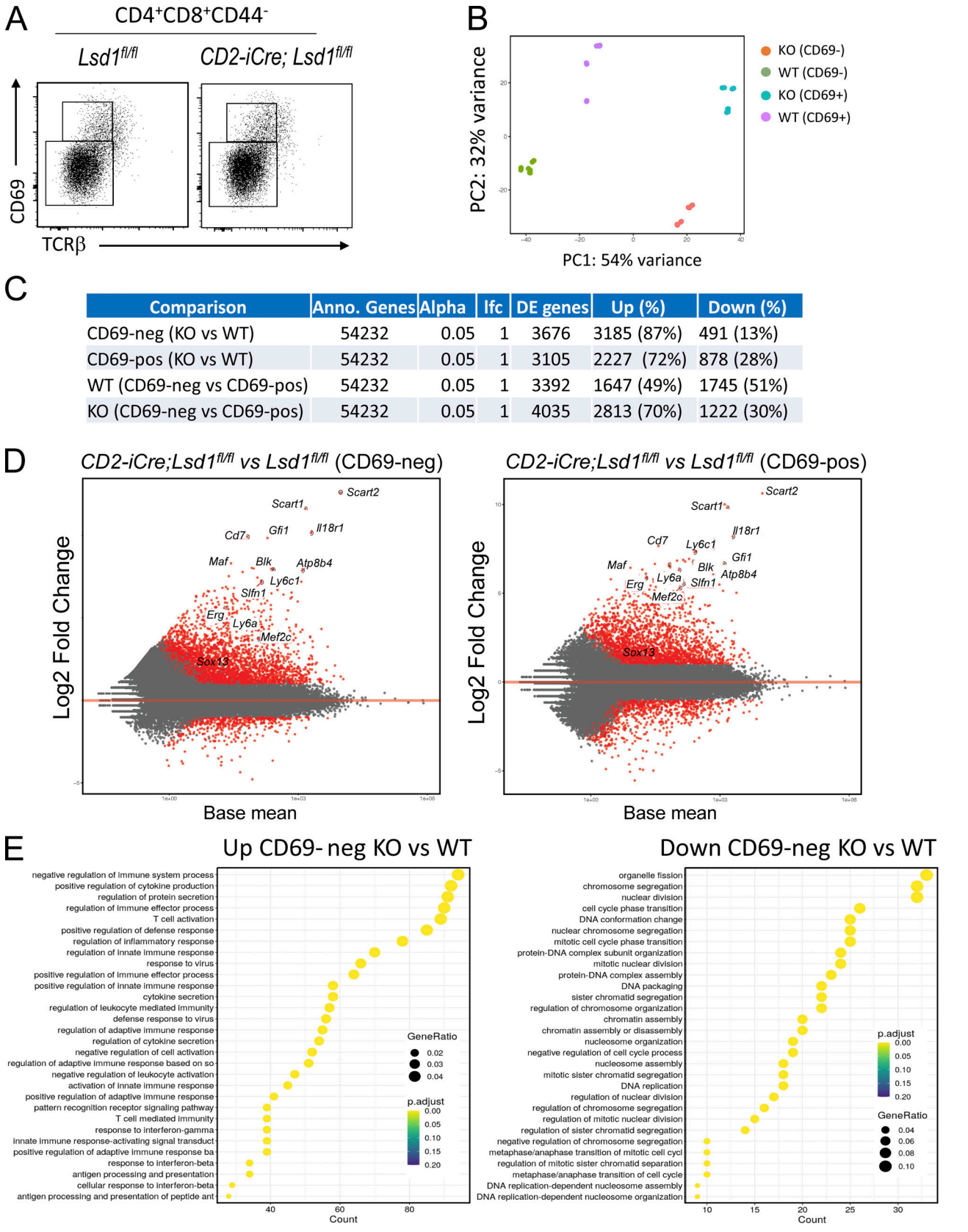

Comparison	Anno. Genes	Alpha	lfc	DE genes	Up (%)	Down (%)
CD69-neg (KO vs WT)	54232	0.05	1	3676	3185 (87%)	491 (13%)
CD69-pos (KO vs WT)	54232	0.05	1	3105	2227 (72%)	878 (28%)
WT (CD69-neg vs CD69-pos)	54232	0.05	1	3392	1647 (49%)	1745 (51%)
KO (CD69-neg vs CD69-pos)	54232	0.05	1	4035	2813 (70%)	1222 (30%)

Figure 3. **Marked gene up-regulation in Lsd1-deficient CD4⁺CD8⁺ (DP) thymocytes. (A)** CD69 versus TCRβ staining profile of gated DP CD44⁻ thymocytes from *Lsd1*$^{fl/fl}$ (WT) and *CD2-iCre;Lsd1*$^{fl/fl}$ (KO) mice showing cell sorting gates used for RNA-seq. **(B)** PCA of RNA-seq results from DP CD69⁻ or DP CD69⁺ thymocytes from *Lsd1*$^{fl/fl}$ and *CD2-iCre;Lsd1*$^{fl/fl}$ mice. **(C)** Results of RNA-seq showing number of up- or down-regulated genes in CD69⁻ and CD69⁺ WT and KO DP thymocytes. Anno., annotated; DE, differentially expressed. lfc, log fold change. **(D)** MA plots showing the predominant up-regulation of genes in DP CD69⁻

and DP CD69+ KO thymocytes. Red dots represent genes that are significantly changed in KO thymocytes. Annotated genes show dysregulation of the same genes in KO CD69− and KO CD69+ DP thymocytes. **(E)** Gene ontology functional enrichment analysis of up-regulated (left) or down-regulated (right) gene sets in CD69− *CD2-iCre;Lsd1*$^{fl/fl}$ thymocytes.

HSC and early DN genes are not extinguished in Lsd1-deficient DP thymocytes

Because a previous study demonstrated an important role for Lsd1 in the down-regulation of stem cell genes during HSC development (Kerenyi et al., 2013), we performed Gene Set Enrichment Analysis (GSEA) on the dysregulated genes in KO CD69− DP thymocytes with the same HSC signature gene sets used in that report (Chambers et al., 2007; Ivanova et al., 2002; Krivtsov et al., 2006). Consistent with the prior study, GSEA revealed a defect in down-regulation of HSC-related genes reflected by overexpression in KO CD69− DP thymocytes (Fig. 4 A). We next examined the effect of Lsd1 deletion on a set of well-characterized HSC-expressed genes that are known to be down-regulated in late-stage DN thymocytes. The HSC-expressed genes *Hoxa7*, *Ly6a* (*Sca1*), *Ptpn3*, and *CD93*, which are normally down-regulated at the DN3/4 stage(s), confirmed by RNA-seq data from https://www.immgen.org (Fig. 4 B), failed to be down-regulated and were strongly overexpressed in *Lsd1* KO CD69− DP thymocytes (Fig. 4 C). Following extinction of HSC-specific genes such as those that regulate self-renewal and long-term maintenance, immature DN thymocytes up-regulate a set of DN stage-specific genes (e.g., *Bcat*, *Pdlim4*, *Ly6c1*, *Ctla4*, *Pld4*, *Pdcd1*, *Nrp1*, and *Tnfrsf8*) that are subsequently down-regulated in DP thymocytes (Fig. 4 D). Similar to HSC genes, DN stage-specific genes failed to be extinguished in *Lsd1* KO DP thymocytes (Fig. 4, C and D). Similar results were observed when we analyzed the effect of *Lsd1* KO on two sets of genes designated *Kit* and *IL7r* (named for the expression pattern of the exemplar gene) that were previously shown to be down-regulated during the DN to DP transition (Mingueneau et al., 2013; Fig. 4 E). We performed a similar analysis of transcription factors previously shown to be either up- or down-regulated during the DN to DP transition (Zhang et al., 2012). Although only a few of the genes that are normally up-regulated as thymocytes transition from DN to DP were affected by deletion of *Lsd1*, a high percentage (120 of 151 [79%]) of genes that are normally down-regulated during the DN to DP transition failed to be repressed in DP thymocytes in the absence of Lsd1 (Fig. 4 F).

We were able to confirm overexpression of several surface molecules by flow cytometry (Fig. 5 A and data not shown). For example, Sca1 was overexpressed on DN, DP, and SP thymocytes as well as mature SP T cells, γδ T cells, and Treg cells in *CD2-iCre;Lsd1*$^{fl/fl}$ mice (Fig. 5 A and data not shown). The checkpoint molecules Pdcd1 (PD-1), Ctla4, and Nrp1, which are expressed in DN thymocytes but are normally down-regulated at the DP stage, were overexpressed on *Lsd1* KO CD69− DP thymocytes, mature CD4+ T cells, and, to a lesser extent, CD8+ T cells (Fig. 5, B and C; and data not shown). Although surface expression of Ctla4 was not markedly elevated on resting *CD2-iCre;Lsd1*$^{fl/fl}$ CD4 T cells, it was strongly induced in response to TCR or TCR + CD28 costimulation (Fig. 5 C). Collectively, these results reveal that deletion of *Lsd1* in DN thymocytes results in the overexpression of HSC and DN stage-specific genes that are normally extinguished by the DP stage.

Another set of genes strongly overexpressed in *Lsd1* KO DP thymocytes were those associated with γδ T cell development (*Scart1*, *Scart2*, *Sox13*, *Maf*, *Blk*; Fig. 3 D). The αβ/γδ lineage fate decision occurs during the DN3 stage of development (Ciofani and Zúñiga-Pflücker, 2010) when Lsd1 expression in *CD2-iCre;Lsd1*$^{fl/fl}$ thymocytes is significantly down-regulated (Fig. 1 A). This finding, which may help explain the increase in γδTCR+ thymocytes in *CD2-iCre;Lsd1*$^{fl/fl}$ mice, suggests that Lsd1 is required to repress γδ lineage signature genes in bipotent αβ/γδ precursors that commit to the αβ lineage and transition to the DP stage.

Alternate hematopoietic lineage genes are expressed in Lsd1-deficient DP thymocytes

DN thymocytes, which are initially multipotent, progressively lose alternate lineage potentials during their maturation in the thymus before irreversibly committing to the αβ T cell lineage. However, it is unknown if repression of alternate lineage genes in DN thymocytes involves or requires epigenetic modifications. To address this question, we examined *Lsd1* KO DP thymocytes for expression of signature myeloid, innate lymphoid, or B cell genes. We found that several alternate lineage genes, including key transcription factors, were aberrantly expressed in *Lsd1* KO CD69− thymocytes, such as *Cebpb*, *Cd11b*, and *Il13ra1* (myeloid), *Fos* and *Klf4* (ILC), *Zbtb16/Plzf*, *Il2rb* and *Prf1* (NK/NKT), and *Ebf1*, *Irf4*, and *Pou2af1* (B cell; Fig. 5 D). Notably, none of these genes is normally expressed in either DN or DP thymocytes, indicating that they were de-repressed in the absence of Lsd1 (Fig. 5 E). We also confirmed that several known target genes of *Cebpb*, *Egr2*, *Zbtb16*, and *Irf4* were significantly dysregulated (overexpressed) in Lsd1 KO DP thymocytes (Fig. S3 B), demonstrating that the increased expression of these transcription factors impacted the expression of downstream genes in *Lsd1* KO DP thymocytes.

To determine if loss of Lsd1 promotes commitment to and/or maturation of alternate hematopoietic lineages, we cultured sorted ETP/DN2 or DN3 thymocytes from *CD2-iCre;Lsd1*$^{fl/fl}$ mice on OP9-DL1 cells for 7 d. No increase in myeloid, B cell, or NK cells was observed in *CD2-iCre;Lsd1*$^{fl/fl}$ thymocyte cultures; however, a reduction in DP thymocytes and an increase in the percentage of γδTCR+ thymocytes was observed, consistent with analysis of thymocytes from adult mice (data not shown). Similar results were obtained when B6 ETP/DN2 or DN3 thymocytes were cultured on OP9-DL1 cells in the presence of the Lsd1 inhibitor GSK-LSD1 (data not shown). These results suggest that although some alternate (non–T cell) lineage genes are expressed in DN/DP thymocytes in the absence of Lsd1, DN thymocytes are not redirected to alternate lineage fates.

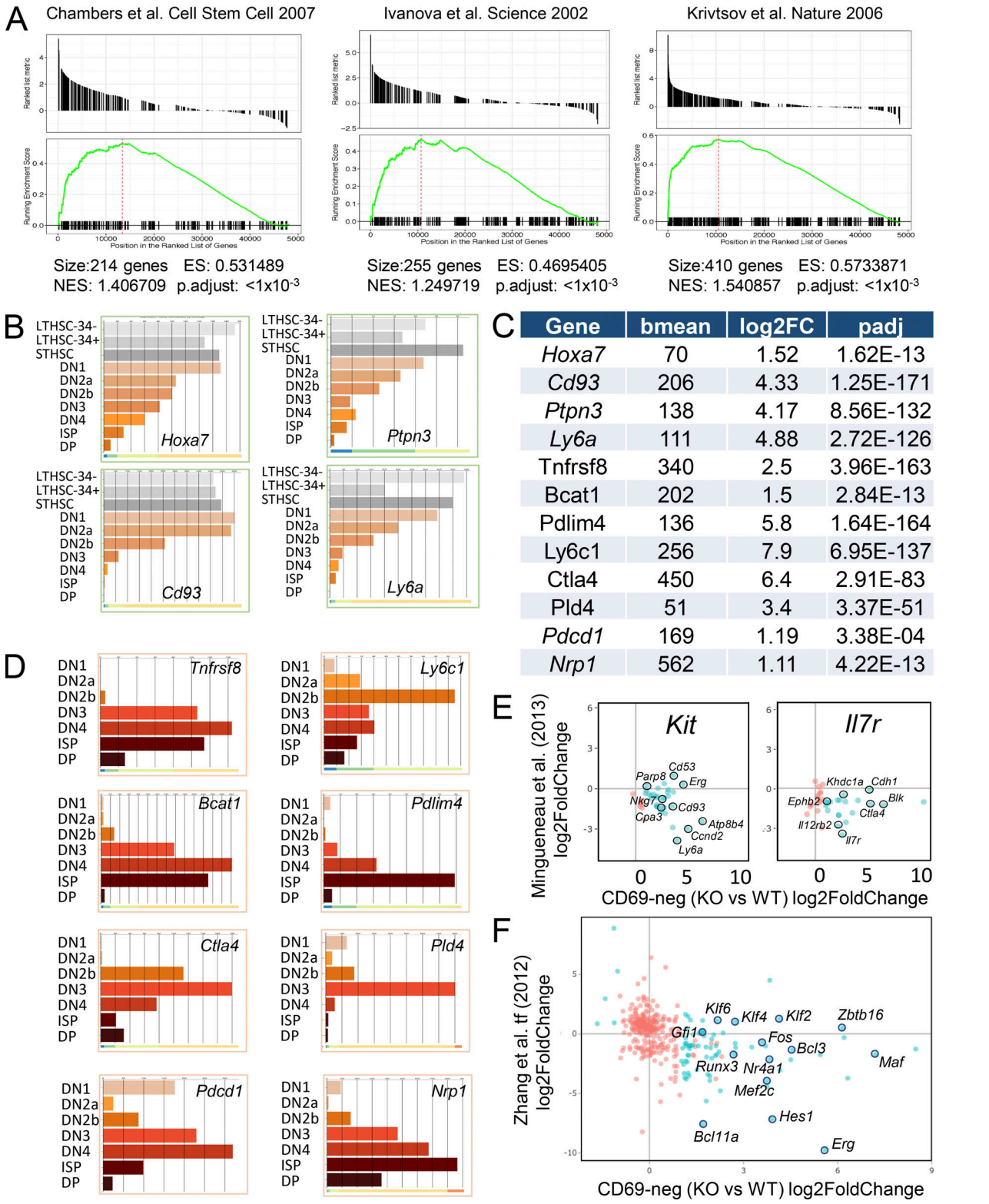

Figure 4. **Overexpression of HSC genes in Lsd1 KO DP thymocytes. (A)** GSEA plots showing enrichment for HSC signature genes in the overexpressed gene set from *CD2-iCre;Lsd1*$^{fl/fl}$ (KO) DP CD69^{-} thymocytes. Genes obtained from Chambers et al. (2007), Ivanova et al. (2002), and Krivtsov et al. (2006). ES, enrichment score; NES, normalized enrichment score. **(B–F)** Effect of Lsd1 deletion on expression of HSC-expressed and DN-specific genes. **(B)** Immgen (https://www.immgen.org) screenshots showing expression of the indicated genes in HSCs (long-term HSC [LTHSC] 34^{-}, LTHSC 34^{+}, short-term HSC [STHSC]), DN thymocyte subsets, ISP thymocytes, or DP thymocytes in WT mice. **(C)** gene expression in *CD2-iCre;Lsd1*$^{fl/fl}$ (KO) versus *Lsd1*$^{fl/fl}$ (WT) CD69^{-} DP thymocytes. Positive $\log_2$FC values indicate that genes are overexpressed in KO thymocytes versus WT thymocytes. **(D)** Immgen screenshots showing expression of the indicated genes listed in C in DN, ISP, or DP thymocytes in WT mice. **(E)** Effect of *Lsd1* deletion on expression of two sets of genes, designated "c-kit" and "Il7r," that are normally down-regulated in DP WT thymocytes compared with DN thymocytes. Genes obtained from Mingueneau et al. (2013).

(F) Effect of Lsd1 deletion on expression of transcription factors that are normally either up- or down-regulated during the DN to DP developmental transition in WT mice. Genes obtained from Zhang et al. (2012). Genes designated in red or blue are nonsignificantly or significantly changed in KO versus WT, respectively. Significance was determined based on the following criteria: FDR <0.05; $\log_2$FC ≤1.

Lsd1 is required for Bcl11b-, Bcl6-, and Gfi1-mediated gene repression

Lsd1 possesses H3K4me1/me2 demethylase activity but lacks DNA binding capability (Hosseini and Minucci, 2017). Several multiprotein complexes, including the chromatin-modifying CoREST and NuRD core complexes, can incorporate Lsd1 in addition to other subunits (typically transcription factors) that provide DNA binding and target specificity (Hosseini and Minucci, 2017). The zinc finger transcription factor Bcl11b, which plays a critical role in T cell development, regulating early events, including T cell commitment and β-selection, as well as controlling gene expression at later stages of thymocyte maturation (Hirose et al., 2015; Kastner et al., 2010; Liu et al., 2010; Wakabayashi et al., 2003), has been shown to associate with NuRD complexes and with Lsd1 (Hosokawa et al., 2018; Le Douce et al., 2012); however, a major role for Lsd1 in Bcl11b-mediated gene repression in thymocytes has not been demonstrated experimentally (Hosokawa et al., 2018). We found that 49 (82%) of 60 previously identified Bcl11b repressed genes, including the transcription factors *Id2* and *Zbtb16* (Hosokawa et al., 2018), were up-regulated in *CD2-iCre;Lsd1*$^{fl/fl}$ CD69$^-$ DP thymocytes (Fig. 6 A), whereas only 3 (4%) of 76 Bcl11b-dependent genes were down-regulated (data not shown), indicating a crucial and selective requirement for Lsd1 for Bcl11b-mediated gene repression. We also observed a striking similarity in the effects of *Bcl11b* or *Lsd1* deletion on the expression of specific transcriptional programs. For example, similar to Bcl11b (Hirose et al., 2015; Kastner et al., 2010), Lsd1 was required for the repression of mature T cell signature genes and for the repression of innate memory T cell–associated genes in DP thymocytes (Fig. 6, B and C). Indeed, as observed in *Bcl11b*-deficient mice (Hirose et al., 2015), *CD2-iCre;Lsd1*$^{fl/fl}$ mice contained a large population of innate-like (CD44$^+$ CD122^{hi} IL-18r$^+$ IL-7ra^{hi} Cxcr3$^+$ CD49d^{lo}) CD8 SP thymocytes (Fig. 6 D) that expressed high levels of Eomes and T-bet and produced IFNγ following stimulation with PMA + ionomycin (Fig. 6 D). Peripheral CD8$^+$ T cells in *CD2-iCre;Lsd1*$^{fl/fl}$ mice were predominantly of the innate memory phenotype (Fig. 7 A), and, as observed in Bcl11b-deficient mice (Albu et al., 2011; Hatano et al., 2017; Kastner et al., 2010), *CD2-iCre;Lsd1*$^{fl/fl}$ mice contained an increased population of innate-like NK1.1$^+$ CD44$^+$ γδTCR$^+$ thymocytes (Fig. 7 B) and a reduced population of NKT cells (Fig. 7 C).

Repressive complexes that include the transcription factors Gfi1 or Bcl6 have also been reported to contain and require Lsd1 for their activity (Hatzi et al., 2019; Saleque et al., 2007). Therefore, we next examined the effect of *Lsd1* deletion on expression of known Gfi1 (Doan et al., 2004; Fraszczak and Möröy, 2021; Li et al., 2010; Shi et al., 2017; van der Meer et al., 2010; Yücel et al., 2003) or Bcl6 (Gioulbasani et al., 2020; Hatzi et al., 2019; Solanki et al., 2020) target genes. Eleven Gfi1 target genes were significantly overexpressed in *Lsd1* KO thymocytes, indicating that Gfi1 repressor activity was lost in the absence of Lsd1 (Fig. 7 D). Indeed, Gfi1, which is autorepressed (Doan et al., 2004), was one of the most highly overexpressed genes in *CD2-iCre;Lsd1*$^{fl/fl}$ DP thymocytes (Fig. 3 D and Fig. 7 D). Interestingly, *S1pr1* was overexpressed in Lsd1-deficient DP thymocytes (Fig. 7 D), which likely contributed, along with the aberrant down-regulation of S1pr1 in SP thymocytes (Fig. 2 E), to the accumulation of mature SP thymocytes in *CD2-iCre;Lsd1*$^{fl/fl}$ mice (Fig. 2 D). A similar effect was observed with the targets of the transcriptional repressor Bcl6, which was recently shown to recruit a CoREST complex containing Lsd1 (Hatzi et al., 2019); specifically, 12 of 17 target genes of Bcl6 were up-regulated in *CD2-iCre;Lsd1*$^{fl/fl}$ CD69$^-$DP thymocytes (Fig. 7 E).

To obtain a more detailed understanding of the effects of Lsd1 deletion on gene expression in thymocytes, we performed single-cell RNA-seq (scRNA-seq) on sorted DN, ISP, and DP thymocytes from *Lsd1*$^{fl/fl}$ and *CD2-iCre;Lsd1*$^{fl/fl}$ mice (Fig. S4, A–C). Uniform Manifold Approximation and Projection (UMAP) plotting of the scRNA-seq data indicated marked differences in the transcriptional profile of control and Lsd1-deficient ISP and DP thymocytes (Fig. 8 A). Notably, we confirmed mis-/overexpression of Bcl11b-dependent genes (Hosokawa et al., 2018), mature SP genes (Chopp et al., 2020), and innate memory genes (Hirose et al., 2015) as well as Bcl6-dependent genes (Gioulbasani et al., 2020) in CD4$^+$CD8$^+$ cells that also expressed a canonical DP gene signature (Chopp et al., 2020; Fig. 8, B–D). In addition, these same genes were found to be mis-/overexpressed in γδ and NKT thymocytes from *Lsd1*-deficient mice (Fig. 8, B–D). Finally, the scRNA-seq data confirmed concurrent mis-/overexpression of these gene sets in CD4$^+$CD8$^+$ cells, showing that they are coexpressed in the same DP thymocytes (Fig. 8 E).

Deletion of *Lsd1* results in enhanced H3K4 trimethylation at promoters of overexpressed genes

To determine if the gene dysregulation in *Lsd1* KO CD69$^-$ DP thymocytes was associated with altered histone 3 methylation, we performed chromatin immunoprecipitation followed by next-generation sequencing (ChIP-seq) on thymocytes from WT (*Lsd1*$^{fl/fl}$) and KO (*CD2-iCre;Lsd1*$^{fl/fl}$) mice with antibodies directed against H3K4me1, H3K4me2, or H3K4me3. Because Lsd1 functions as a histone demethylase, we looked for sites where H3K4me1, H3K4me2, and H3K4me3 marks were increased in KO versus WT thymocytes. Peak analysis of the differentially decorated sites revealed that only H3K4 trimethylated sites were significantly increased in KO thymocytes (Fig. 9 A). Also, only a small fraction (1.8%) of the total consensus H3K4 trimethylated sites (sites present in both WT and KO thymocytes) were significantly ($P < 0.01$) different in WT and KO thymocytes, indicating that the effect of *Lsd1* deletion was restricted to a relatively small set of genes (Fig. 9 A). The majority (222 of 293 [76%]) of the enhanced H3K4me3 sites were located at presumptive gene promoters (≤1 kb from the transcription start site), and enhanced H3K4 trimethylation at gene promoters

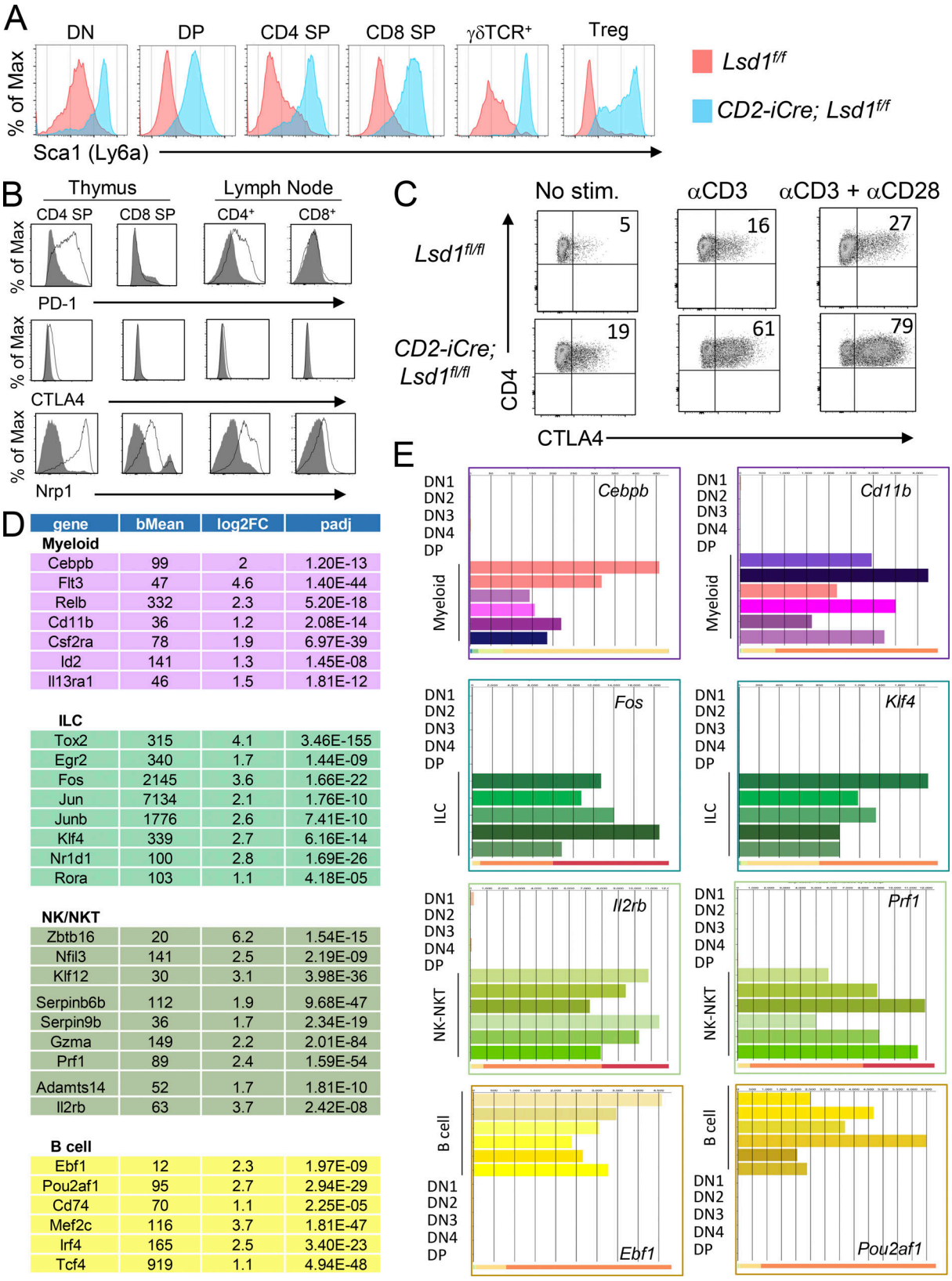

D

gene	bMean	log2FC	padj
Myeloid			
Cebpb	99	2	1.20E-13
Flt3	47	4.6	1.40E-44
Relb	332	2.3	5.20E-18
Cd11b	36	1.2	2.08E-14
Csf2ra	78	1.9	6.97E-39
Id2	141	1.3	1.45E-08
Il13ra1	46	1.5	1.81E-12
ILC			
Tox2	315	4.1	3.46E-155
Egr2	340	1.7	1.44E-09
Fos	2145	3.6	1.66E-22
Jun	7134	2.1	1.76E-10
Junb	1776	2.6	7.41E-10
Klf4	339	2.7	6.16E-14
Nr1d1	100	2.8	1.69E-26
Rora	103	1.1	4.18E-05
NK/NKT			
Zbtb16	20	6.2	1.54E-15
Nfil3	141	2.5	2.19E-09
Klf12	30	3.1	3.98E-36
Serpinb6b	112	1.9	9.68E-47
Serpin9b	36	1.7	2.34E-19
Gzma	149	2.2	2.01E-84
Prf1	89	2.4	1.59E-54
Adamts14	52	1.7	1.81E-10
Il2rb	63	3.7	2.42E-08
B cell			
Ebf1	12	2.3	1.97E-09
Pou2af1	95	2.7	2.94E-29
Cd74	70	1.1	2.25E-05
Mef2c	116	3.7	1.81E-47
Irf4	165	2.5	3.40E-23
Tcf4	919	1.1	4.94E-48

Figure 5. **Up-regulation of HSC, DN stage-specific, and alternate lineage genes and checkpoint proteins in thymocytes and T cells in *CD2-iCre;Lsd1$^{fl/fl}$* mice. (A)** Overexpression of the HSC surface protein Sca1 (Ly6a) on thymocytes and T cells from *CD2-iCre;Lsd1$^{fl/fl}$* mice. **(B)** Surface staining showing overexpression of PD-1, Ctla4, and Nrp1 on CD4 SP and CD8 SP thymocytes and T cells from *CD2-iCre;Lsd1$^{fl/fl}$* mice. Shaded, *Lsd1$^{fl/fl}$*; black line, *CD2-iCre;Lsd1$^{fl/fl}$*. **(C)** Intracellular staining showing induced expression of Ctla4 in CD4$^+$ T cells from *Lsd1$^{fl/fl}$* or *CD2-iCre;Lsd1$^{fl/fl}$* mice after stimulation with antibodies against CD3 ± CD28 in the presence of APCs. **(D)** Expression of "alternate lineage" (myeloid cell, ILC, NK cell, NKT cell, or B cell) genes in Lsd1 KO (*CD2-iCre;Lsd1$^{fl/fl}$*) CD69$^-$ thymocytes. **(E)** Immgen screenshots showing expression of the indicated alternate lineage genes in WT thymocytes or WT cells of the indicated lineage. Note absence of expression in DN or DP thymocytes. Results shown in A–C are representative of three or more experiments.

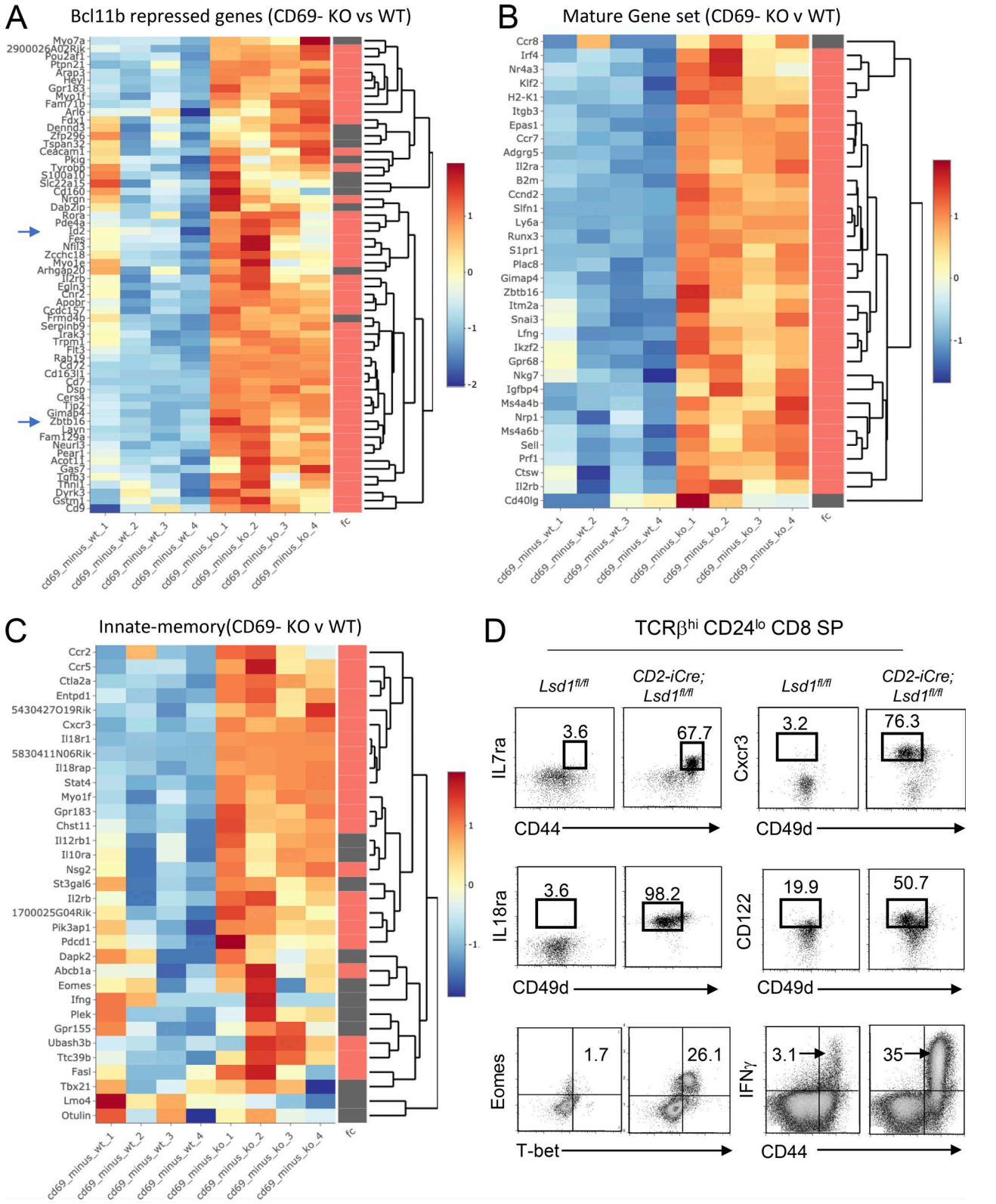

Figure 6. **Lsd1-deficient and Bcl11b-deficient thymocytes exhibit similar gene overexpression profiles and phenotypes. (A)** Heatmap comparing expression of Bcl11b-repressed genes in CD69⁻ DP thymocytes from control, *Lsd1*$^{fl/fl}$, and *CD2-iCre;Lsd1*$^{fl/fl}$ mice. Bcl11b-repressed genes are from Hosokawa et al. (2018). Significantly overexpressed genes are designated by red bars in the last column. Arrows designate the key Bcl11b-repressed transcription factors Id1 and Zbtb16. **(B)** Heatmap comparing expression of mature T cell–restricted genes in CD69⁻ DP thymocytes from control, *Lsd1*$^{fl/fl}$, and *CD2-iCre;Lsd1*$^{fl/fl}$ mice. **(C)** Heatmap comparing expression of innate memory genes in CD69⁻ DP thymocytes from control, *Lsd1*$^{fl/fl}$, and *CD2-iCre;Lsd1*$^{fl/fl}$ mice. **(D)** Innate memory phenotype of CD8 SP thymocytes from *CD2-iCre;Lsd1*$^{fl/fl}$ mice. One representative of two experiments is shown.

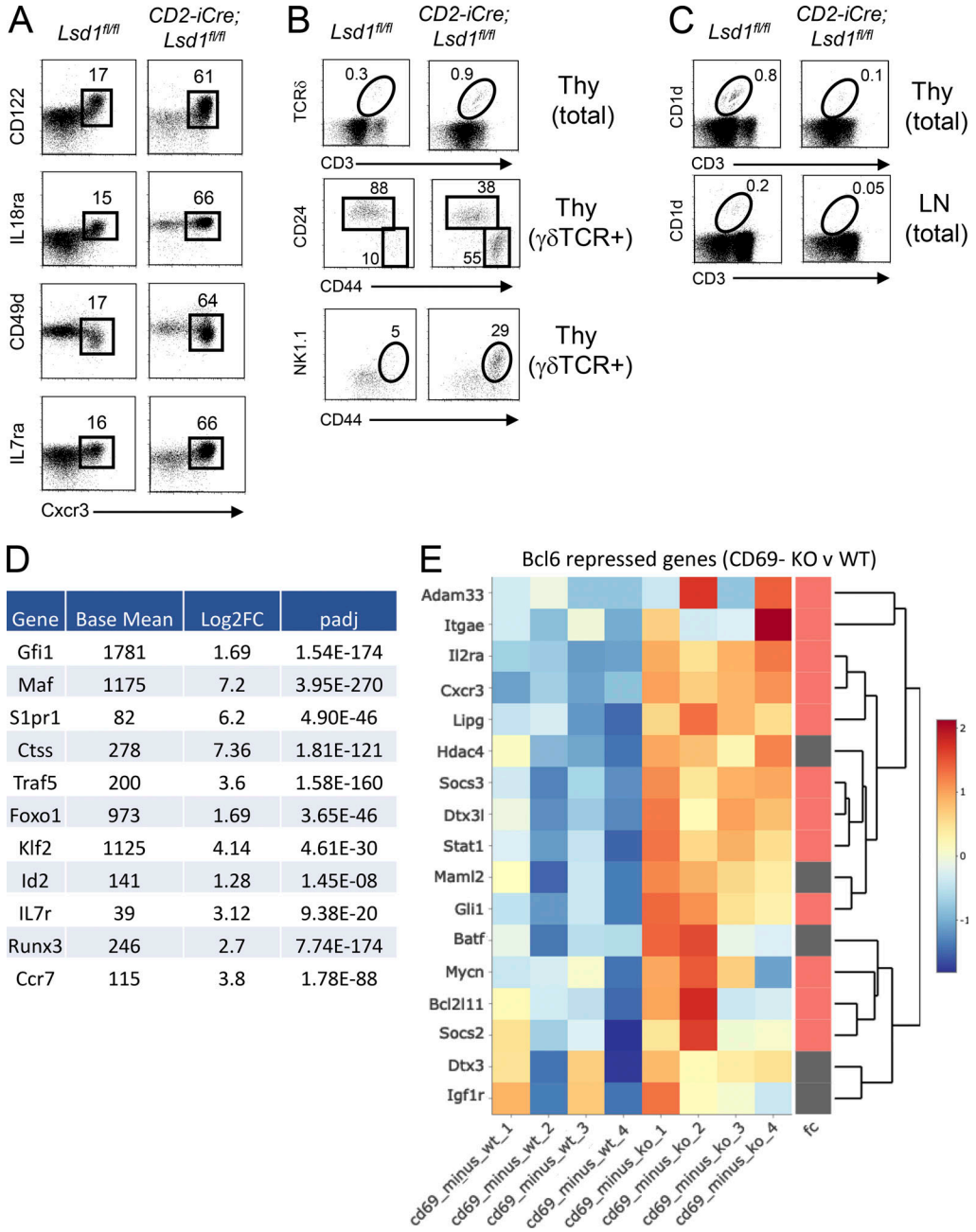

Gene	Base Mean	Log2FC	padj
Gfi1	1781	1.69	1.54E-174
Maf	1175	7.2	3.95E-270
S1pr1	82	6.2	4.90E-46
Ctss	278	7.36	1.81E-121
Traf5	200	3.6	1.58E-160
Foxo1	973	1.69	3.65E-46
Klf2	1125	4.14	4.61E-30
Id2	141	1.28	1.45E-08
IL7r	39	3.12	9.38E-20
Runx3	246	2.7	7.74E-174
Ccr7	115	3.8	1.78E-88

Figure 7. **Phenotype of *CD2-iCre;Lsd1$^{fl/fl}$* mice resembles Bcl11b-deficient mice. (A)** Innate memory phenotype of peripheral CD8$^+$ T cells in LN from *CD2-iCre;Lsd1$^{fl/fl}$* mice. **(B)** Presence of NK1.1$^+$ γδ T cells in the thymus of *CD2-iCre;Lsd1$^{fl/fl}$* mice. **(C)** Reduction in NKT cells in *CD2-iCre;Lsd1$^{fl/fl}$* mice. For A–C, one representative of two experiments is shown. **(D)** Effect of *Lsd1* deletion on expression of *Gfi1*-repressed genes. Shown are gene expression in *CD2-iCre;Lsd1$^{fl/fl}$* (KO) CD69$^-$ DP thymocytes. (Positive $\log_2$FC values indicate that genes are overexpressed in KO thymocytes versus WT thymocytes.) **(E)** Heatmap comparing expression of Bcl6-repressed genes in CD69$^-$ DP thymocytes from control, *Lsd1$^{fl/fl}$*, and *CD2-iCre;Lsd1$^{fl/fl}$* mice. Significantly overexpressed genes are designated by red bars in the last column.

correlated with transcriptional up-regulation in CD69$^-$ KO DP thymocytes (Fig. 9 B).

Screening of the genes with enhanced H3K4 trimethylation that are overexpressed in DP thymocytes using the University of California, Santa Cruz (UCSC) Genome Browser revealed that although H3K4me1 and H3K4me2 decoration was frequently also increased, this was not a consistent trend (Fig. S4, D and E). The enhanced H3K4 trimethylation observed in KO thymocytes was not due to misexpression of known H3K4 methyltransferases or other H3K4 demethylases, because, with the exception of *Kdm5a*, which was slightly decreased in CD69$^-$ KO DP thymocytes, expression of these genes was either unaffected or altered in a manner not predicted to predispose to increased H3K4 methylation (data not shown).

Mining of the ChIP-seq data identified three gene clusters that appear to be epigenetically coregulated. The γδ lineage-

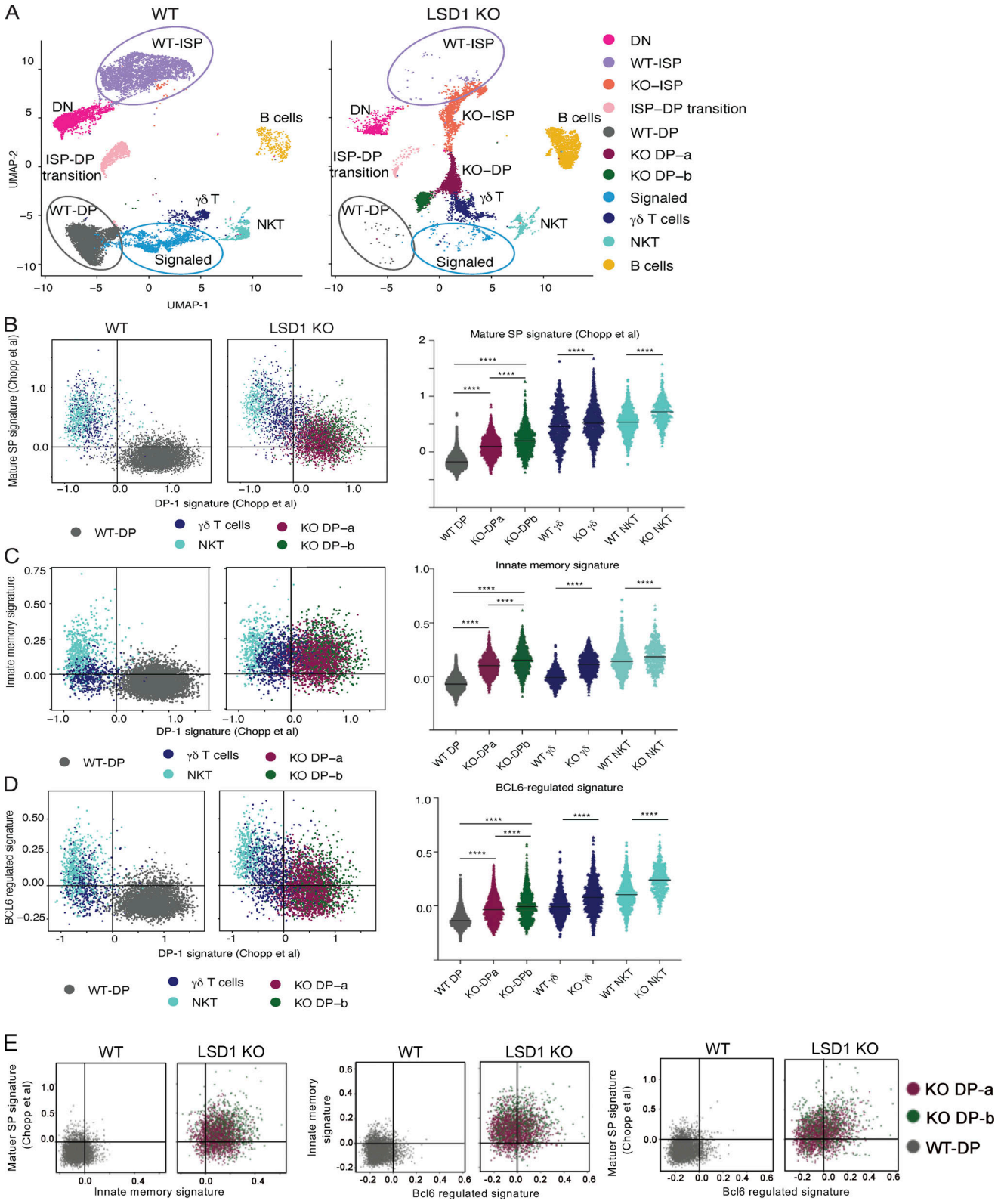

Figure 8. **Marked gene expression differences in control and Lsd1-deficient DP thymocytes revealed by scRNA-seq. (A)** UMAP plot of scRNA-seq in thymocytes from control, *Lsd1*$^{fl/fl}$, and *CD2-iCre;Lsd1*$^{fl/fl}$ mice. Thymocytes are color coded according to their distribution into clusters (names shown on right). **(B–D)** Left: scRNA-seq data for (B) mature SP signature genes, (C) innate memory signature genes, or (D) Bcl6-regulated (repressed) genes plotted versus DP-1 (CD69^{-}) signature genes. Gene lists are provided in Data S1. Right: Violin plots show cluster-based average expression scores of the indicated gene sets. ****, $P < 0.001$; significance determined using an ordinary one-way ANOVA followed by Šidák's multiple comparisons test. **(E)** Plots of scRNA-seq data on gated DP thymocytes for the indicated signature gene sets showing coexpression in the same DP cells.

A

Mark	Consensus sites	Up (KO vs WT)	Down (KO vs WT)	Changed (KO vs WT)
H3K4me1	24849	147 (42%)	205 (58%)	352
H3K4me2	25263	213 (39%)	338 (61%)	551
H3K4me3	15330	279 (95%)	14 (5%)	293

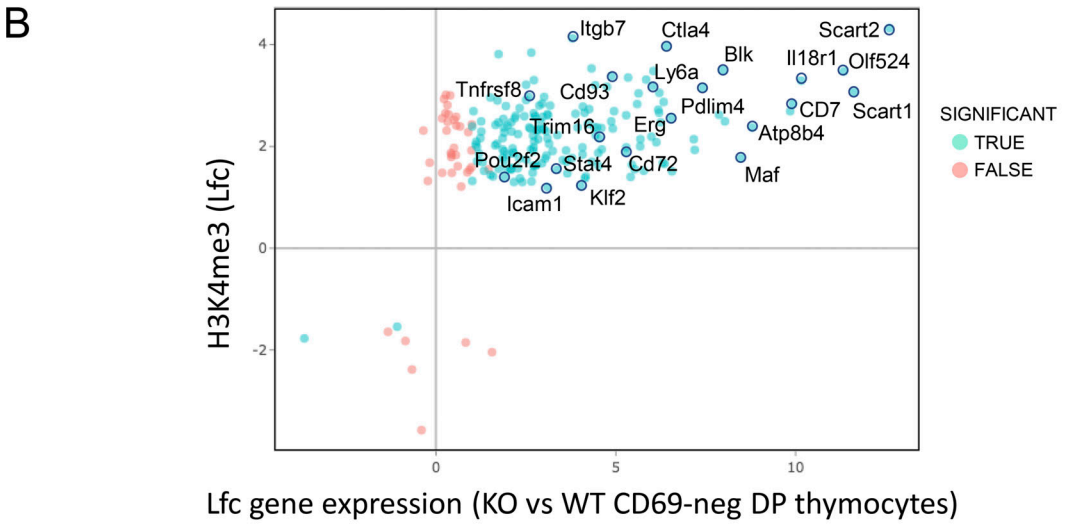

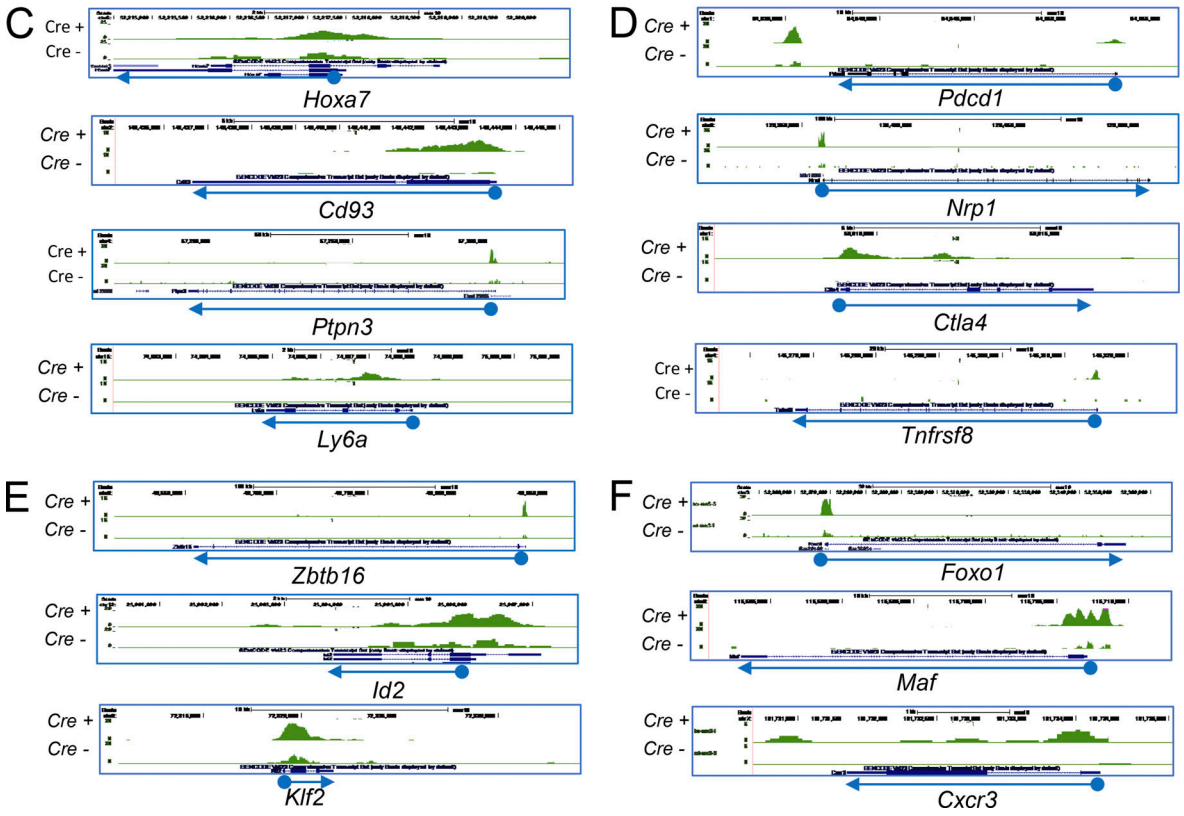

Figure 9. **Gene overexpression in *CD2-iCre;Lsd1$^{fl/fl}$* CD69^{-} DP thymocytes is associated with enhanced H3K4 trimethylation at gene promoters. (A)** Number and type of H3K4 methylation marks in *Lsd1$^{fl/fl}$* versus *CD2-iCre;Lsd1$^{fl/fl}$* thymocytes obtained by ChIP-seq with anti-H3K4me1, 2, or 3 antibodies. Shown are total consensus H3K4me1, 2, or 3 sites in *Lsd1$^{fl/fl}$* (WT) and *CD2-iCre;Lsd1$^{fl/fl}$* (KO) thymocytes, and the number of sites where decoration is significantly increased (Up), decreased (Down), or changed (Up or Down) in KO versus WT thymocytes. **(B)** Scatter plot of H3K4me3 intensity at gene promoters versus logarithmic fold change (Lfc) gene expression (KO versus WT) in CD69^{-} DP thymocytes. Genes designated in red or blue are nonsignificantly or significantly changed in KO versus WT, respectively. Significance was determined based on the following criteria: FDR <0.05; $\log_2$FC ≤1. **(C–F)** UCSC Genome Browser screenshots of H3K4me3 decoration at the promoters of (C) HSC-expressed genes in DP thymocytes from *Lsd1$^{fl/fl}$* (Cre^{-}) or *CD2-iCre;Lsd1$^{fl/fl}$* (Cre^{+}) mice, (D) DN stage-specific genes in DP thymocytes from *Lsd1$^{fl/fl}$* (Cre^{-}) or *CD2-iCre;Lsd1$^{fl/fl}$* (Cre^{+}) mice, (E) Bcl11b-repressed genes in DP thymocytes from *Lsd1$^{fl/fl}$* (Cre^{-}) or *CD2-iCre;Lsd1$^{fl/fl}$* (Cre^{+}) mice, and (F) Gfi1-repressed (*Foxo1*, *Maf*) or Bcl6-repressed (*Cxcr3*) genes in DP thymocytes from *Lsd1$^{fl/fl}$* (Cre^{-}) or *CD2-iCre;Lsd1$^{fl/fl}$* (Cre^{+}) mice.

specific genes *Scart1* (*CD3163l1*) and *Scart2* (*5830411N06Rik*), each of which is strongly overexpressed in *Lsd1* KO DP thymocytes (Fig. 3 D and data not shown), are closely linked on chromosome 7. The promoters and gene bodies of *Scart1* and *Scart2* in KO but not WT DP thymocytes were decorated with H3K4me3 (as well as H3K4me1 and H3K4me2) marks (data not shown). H3K4me1, H3K4me2, and H3K4me3 decoration was also observed at the nearby gene *Olfr524* specifically in KO thymocytes, and *Olfr524* was strongly overexpressed in *Lsd1* KO DP thymocytes (data not shown). Moreover, *Olfr524* exhibited an expression pattern similar to that of *Scart1* and *Scart2* in WT DN thymocytes. We detected two additional coregulated gene clusters: *Itgb7-Rarg* on chromosome 15 and *March9-Cdk4-Tspan31* on chromosome 10 (data not shown). In both cases, each gene in the cluster was overexpressed in KO DP thymocytes and was overdecorated with H3K4me3 (data not shown).

The promoters of the HSC signature genes (e.g., *Hoxa7*, *Cd93*, *Ptpn3*, and *Ly6a* [*Sca1*]) that failed to be down-regulated in *CD2-iCre;Lsd1*$^{fl/fl}$ DP thymocytes (Fig. 4 C) were more highly decorated with H3K4me3 than control *Lsd1*$^{fl/fl}$ DP thymocytes (Fig. 9 C). Likewise, promoters of the DN stage-specific genes *Pdcd1*, *Nrp1*, *Ctla4*, and *Tnfrsf8* were marked with H3K4me3 in *CD2-iCre;Lsd1*$^{fl/fl}$ DP thymocytes but not *Lsd1*$^{fl/fl}$ DP thymocytes (Fig. 9 D). As expected, the promoters of several HSC genes that were strongly down-regulated in both WT (*Lsd1*$^{fl/fl}$) and KO (*CD2-iCre;Lsd1*$^{fl/fl}$) thymocytes (e.g., *Hoxa9*, *Gata2*, and *Tal1*) were devoid of H3K4me3 marks (Fig. S5, A and B). Interestingly, the promoters of several other HSC-expressed genes that were strongly down-regulated in DP thymocytes were decorated with H3K4me3 in both *Lsd1*$^{fl/fl}$ and KO *CD2-iCre;Lsd1*$^{fl/fl}$ DP thymocytes, demonstrating that H3K4 trimethylation is not sufficient for the expression of these genes (Fig. S5, A and C).

We also found that the Bcl11b-repressed genes *Zbtb16*, *Id2*, and *Klf2* were strongly decorated with H3K4me3 in Lsd1-deficient thymocytes but not control thymocytes, consistent with a requirement for Lsd1 for Bcl11b-mediated repression of these genes (Fig. 9 E). Finally, we documented enhanced H3K4me3 decoration at the promoters of genes known to be repressed by Gfi1 (Foxo1, *Maf*) or Bcl6 (*Cxcr3*) in Lsd1-deficient DP thymocytes, consistent with a requirement for Lsd1 for the repression of these genes (Fig. 7, D and E; and Fig. 9 F).

Discussion

Studies investigating the role of epigenetic modification during T cell development as a mechanism for silencing gene expression have focused primarily on the deposition of inhibitory H3K27 trimethylation (Rothenberg and Zhang, 2012; Tanaka et al., 2013; Zhang et al., 2012). Those studies have shown that whereas promoter H3K27 trimethylation is frequently associated with gene repression, a large number of repressed genes lack H3K27me3 marks, and H3K27 methylation appears to control limited functions in DN thymocytes such as cell proliferation rather than serving as a mechanism for widespread repression of stem cell and alternate lineage genes (Miyazaki et al., 2008; Zhang et al., 2012). Previous reports have also shown an important role for removal of activating H3K4 methyl marks as a mechanism for extinguishing expression of early pluripotent genes in embryonic stem cells in HSCs during myelopoiesis by inhibiting or deleting the H3K4me1,2-specific demethylase Lsd1 (Kdma1; Kerenyi et al., 2013; Sprüssel et al., 2012; Whyte et al., 2012). Using a similar (conditional deletion) strategy of T lineage–restricted *Lsd1* deletion, we investigated the importance of Lsd1 and, by extension, H3K4 demethylation as a mechanism for regulating gene expression during early T cell development. Our results identify a critical role for Lsd1 in the down-regulation of HSC genes, confirming previous findings (Kerenyi et al., 2013), and they also reveal, for the first time, a function for Lsd1 in extinguishing expression of early gene programs that are selectively active in DN thymocytes or in alternate hematopoietic lineages, as well as establishing a key role for Lsd1 in the regulation of genes repressed by the transcription factors Bcl11b, Gfi1, and Bcl6.

Deletion of *Lsd1* in DN thymocytes resulted in an incomplete block in T cell development at the DN to DP transition that was accompanied by the continued expression of HSC and DN stage-specific genes that are normally down-regulated by the DP stage as well as aberrant expression of several alternate lineage genes. However, deletion or inhibition of Lsd1 did not result in lineage divergence, indicating that inductive events are required in addition to loss of Lsd1-mediated gene repression for lineage diversion of DN thymocytes or that the level of expression of alternate lineage genes is not sufficient to initiate diversion. Peripheral CD4$^+$ and CD8$^+$ T cell numbers were strongly reduced in *Lsd1* KO mice, indicating a block in terminal SP thymocyte development. Considering the striking gene dysregulation observed in *Lsd1* KO DP thymocytes, it is perhaps surprising that subsequent steps of thymocyte maturation can be successfully navigated and that mature T cells are capable of functional responses such as proliferation and cytokine production. However, we could not establish precisely when Lsd1 deletion occurred in individual cells that progress past the DP stage. Only a small percentage of DP thymocytes successfully complete the selection process, and it is possible that those cells delete *Lsd1* at later stages than the bulk of DP thymocytes, possibly due to strong selective pressure against deletion. For that reason, we did not conduct an extensive evaluation of mature T cell responses or attempt to draw conclusions regarding the impact of Lsd1 deficiency on mature T cell functions.

A notable effect of *Lsd1* deletion on thymocyte development was the loss of Bcl11b-mediated gene repression (Hosokawa et al., 2018), which resulted in a phenotype that closely resembled that of conditional *Bcl11b*-deficient thymocytes, including the de-repression of mature T cell signature genes, the generation of innate-like CD8 SP thymocytes and NK1.1$^+$ γδ T cells, and a reduction in NKT cells (Albu et al., 2011; Hatano et al., 2017; Hirose et al., 2015; Kastner et al., 2010). The remarkable phenotypic similarity of Lsd1-deficient and Bcl11b-deficient thymocytes likely reflects the prominent role of Bcl11b in T cell development. Although Lsd1 had been detected as a subunit of Bcl11b/NuRD repressive complexes (Hosokawa et al., 2018; Le Douce et al., 2012), a major role for Lsd1 activity had not previously been demonstrated. For example, a recent report found that <15% of genes repressed by Bcl11b were up-regulated

following deletion of *Lsd1* in DN thymocytes (Hosokawa et al., 2018). The discrepancy between those results and our own, which identify a critical and pervasive function for Lsd1 in Bcl11b-mediated gene repression, may be the relatively late loss of Bcl11b protein expression in the prior study, which used CRISPR to inactivate *Lsd1* in DN thymocytes (Hosokawa et al., 2018). We also provide evidence that Lsd1 is required for the activity of Gfi1 and Bcl6 repressive complexes during T cell maturation, and we detected de-repression of several transcription factors previously reported to be Gfi1 (*Maf*, *Foxo1*, *Klf2*) or Bcl6 (Mycn, Stat1) targets as well several other known Gfi1 or Bcl6 target genes. Together, these results establish Lsd1 as a key factor used by several different repressive complexes during T cell development.

A previous study found that deletion of *Lsd1* in HSCs results in accumulation of H3K4me1 and H3K4me2 marks at the promoters of several key HSC genes and is associated with failure to repress those genes (Kerenyi et al., 2013). In contrast, we found no strong association between increased H3K4me1 or H3K4me2 promoter decoration and gene expression in *Lsd1* KO thymocytes. Instead, many genes that failed to be repressed in *Lsd1* KO DP thymocytes consistently exhibited only enhanced decoration with H3K4me3 marks. Thus, in thymocytes, it appears that in the absence of Lsd1-mediated H3K4me1,2 demethylation, H3K4 mono- or dimethylation marks are converted to activating H3K4me3 marks. It is notable that whereas >3,000 genes were overexpressed in *Lsd1*-deficient CD69^{-} DP thymocytes, <300 genes were H3K4me3 hypermethylated, representing <2% of all H3K4me3 decorated genes in DP thymocytes. This suggests that much of the gene overexpression observed in *Lsd1* KO DP thymocytes is not a direct result of H3K4 hypermethylation but rather results from indirect effects. For example, *Mef2c*, *Stat5b*, and *Runx3* did not exhibit evidence of increased H3K4me3 decoration but were strongly up-regulated in Lsd1-deficient thymocytes. The apparent cascade effect on gene expression from deletion of *Lsd1* may be due to failure to extinguish the expression of a relatively small number of critical transcription factors with documented repressor activity (e.g., Bcl11b, Gfi1, Bcl6), resulting in dysregulation of their target genes in the absence of altered epigenetic modifications at those genes. Particularly notable is that *Zbtb16* and *Id2*, which are direct targets of Bcl11b, were overexpressed in *Lsd1*-deficient thymocytes, and the promoters of these genes were overdecorated with H3K4me3 marks. Both genes have been shown to regulate distinct and essential gene programs in thymocytes (Hosokawa et al., 2018), and their de-repression in *Lsd1*-deficient thymocytes would be predicted to affect the expression of these target genes. Another consideration is that Lsd1 has been reported to perform functions independent of its H3K4 demethylase activity, such as by regulating the stability/turnover of other proteins and to contribute to gene activation by removing K370 or H3K9 methylation marks (Huang et al., 2007; Perillo et al., 2020). Although the latter activity has only been demonstrated in the context of the androgen receptor, it remains possible that some of the effects observed in *Lsd1*-deficient thymocytes, perhaps accounting for the instances of gene repression in the absence of Lsd1, are due to functions unrelated to H3K4 demethylase activity.

We also found that, at least in some instances, H3K4me3 promoter decoration is not sufficient for gene expression, because several HSC genes, including *Lmo2*, *Lyl1*, and *Hhex*, were strongly down-regulated despite H3K4me3 promoter decoration. It is possible that these promoters are also marked with H3K27me3 and are "bivalent" (i.e., H3K4me3/H3K27me3 dual marked). Bivalent marking has been associated with an inactive but "poised" transcriptional state (Bernstein et al., 2006; Vastenhouw and Schier, 2012). These results reveal that the repression of some genes does not require removal of H3K4me3 marks or continuous expression of Lsd1 after they are extinguished.

Due to different experimental approaches, we were unable to directly compare the effects of loss of H3K4me1 and H3K4me2 demethylase activity (through deletion of *Lsd1*) with loss of H3K27me3 demethylase activity (through deletion of *Utx* and *Jmjd3*; Manna et al., 2015). Whereas our approach resulted in loss of *Lsd1* in mid/late-stage DN thymocytes, thereby impacting the DN to DP transition, deletion of *Utx* and *Jmjd3* was mediated by *CD4-Cre*, which results in deletion at the DP stage (Manna et al., 2015). The main impact of *Lsd1* deletion manifested at the DP stage; however, it remains unclear if the overexpression of HSC and DN stage-specific genes also requires changes in H3K27 methylation, specifically removal of H3K27 promoter marks. Deletion of *Utx* and *Jmjd3* at the DP stage resulted in up-regulation of a limited set of genes, including some (e.g., *S1pr1* and *Klf2*) that function primarily to regulate late stages of thymocyte maturation and thymocyte emigration. Interestingly, all of the genes that were dysregulated (down-regulated) in *Utx/Jmjd3* compound deletion mutants, namely *S1pr1*, *Klf2*, *Ccnd2*, *Irf4*, *Il6ra*, *Foxo1*, and *Lfng*, were strongly overexpressed in *CD2-iCre; Lsd1*$^{fl/fl}$ DP thymocytes, indicating that they are also regulated by Lsd1.

In conclusion, the results reported here establish Lsd1 as a major factor used during T cell development for gene repression. Lsd1 is overexpressed in many cancer cells, and Lsd1 inhibitors have been developed as promising chemotherapeutic agents. Our results thus raise important considerations concerning the potential "off-target" effects of these inhibitors, particularly in younger individuals where T cell development is ongoing.

Materials and methods

Mice

Lsd1$^{fl/fl}$ mice were obtained from M. Rosenfeld (Wang et al., 2007). *hCD2-iCre* and *CD4-Cre* transgenic mice were obtained from The Jackson Laboratory and Taconic Farms, respectively. *Rag1-Cre* transgenic mice were kindly provided by Terence Rabbitts (University of Oxford, Oxford, UK). All procedures were approved by the National Institute of Child Health and Human Development (NICHD) Animal Care and Use Committee.

Flow cytometry

Whole thymi were dissected and processed. Thymocytes were counted and were incubated with 2.4G2 blocking antibody (BE0307; Bio X Cell) for 10 min in the dark at room temperature, washed, then stained with fluorescent conjugated antibodies for

20 min in the dark at room temperature. The following antibodies were used for flow cytometry, all from BD Biosciences unless otherwise noted: CD3e (145-2C11), CD4 (RM4-5), CD8a (53-6.7), CD24 (M1/69), CD25 (PC61), TCRβ (H57-597), TCRγδ (GL3), CD44 (IM7), CD49d (R1-2), CD62L (MEL-14), CD69 (H1.2F3), CD122 (TM-b1; eBioscience), IL7ra/CD127 (SB/199), IL18ra/CD218a (A17071D; BioLegend), Cxcr3/CD183 (Cxcr3-173), NK1.1 (PK136; eBioscience), CD1d (National Institutes of Health Tetramer Core Facility), Sca-1/Ly-6A/E (D7), c-Kit (2B8), PD-1/CD279 (29F.1A12; BioLegend), CTLA4/CD152 (UC10-4F10-11), Nrp1/CD304 (3E12; BioLegend), IFNγ (XMG1.2; eBioscience), GzmB (GB12; eBioscience), T-bet (4B10; eBioscience), and Eomes (Dan11mag; eBioscience). For lineage-negative thymocyte analysis, cells were incubated with the following biotinylated antibodies: CD4 (RM4-5), CD8a (53-6.7), TCRβ (H57-597), TCRγδ (GL3), CD11b/Mac-1 (M1/70), CD11c (HL3), CD19 (1D3), B220 (RA3-6B2), Gr1 (RB6-8C5), Ter119, CD49b (Dx5), NK1.1 (PK136), all from BD Biosciences. Cells were then stained with a streptavidin-conjugated Qdot 605 secondary antibody (Q10101MP; Invitrogen). Data were acquired on an LSR II flow cytometer (BD Biosciences) and analyzed using FlowJo software (BD Biosciences).

Intracellular staining and cell cycle analysis

For intracellular Lsd1 staining, after cells were stained for surface markers, cells were fixed and permeabilized using an eBioscience FoxP3/Transcription Factor Staining Buffer Set (00-5523-00). Then cells were incubated with a rabbit anti-Lsd1 antibody (2139s; Cell Signaling Technology) at room temperature in the dark for 30 min, washed, then stained with an Alexa Fluor 647–conjugated goat anti-rabbit secondary antibody (A27040; Invitrogen) for 30 min in the dark at 4°C. A similar procedure was followed for FoxP3 intracellular staining, except that the FoxP3 antibody was directly fluorescent antibody conjugated (FJK-16s; eBioscience). For cell cycle analysis, after surface staining, fixation, and permeabilization, cells were stained with Ki-67 (561126; BD Biosciences) and DAPI (D21490; Invitrogen) on wet ice. Data were then acquired on an LSR II flow cytometer.

Functional assays

A 96-well plate was coated with anti-CD3ε (145-2C11; Bio X Cell) antibodies at the following concentrations: 0 µg/100 µl, 0.2 µg/100 µl, 0.4 µg/100 µl, 0.6 µg/100 µl, and 0.8 µg/100 µl. Splenocytes and LN cells were incubated with ammonium-chloride-potassium lysing buffer (A10492-01; Gibco) to remove RBCs. A mixture of biotinylated antibodies (B220, 1:250 final; CD11b, 1:250 final; NK1.1, 1:200 final; CD44, 1:500 final; Ter119, 1:250 final; TCRγδ, 1:250 final; and 2.4G2 blocking, 1:100 final) were added to the cell suspension, followed by streptavidin bead incubation. Non-T cells were then removed by passing the cell preparation through a magnetic LS column (130-042-401; Miltenyi Biotec). The purified T cells were plated at a concentration of 2×10^5 cells/200 µl and incubated for 3 d in the presence or absence of 1 µg/ml of anti-CD28 antibody (37.51; Bio X Cell). Then $CD4^+$ and $CD8^+$ T lymphocytes were assessed for cell surface expression of CD69. For proliferation and cytokine production assays, LN T cells and APCs were purified from total LNs and spleens, respectively. Purified T cells (2×10^5) and irradiated APCs (10^6) were cocultured in media containing IL2 (10 ng/ml, 212-12; PeproTech), anti-CD3e (145-2C11; eBioscience), and anti-CD28 (37.51; BioLegend) at the indicated concentrations. For the proliferation assay, T cells were stained with CellTrace Violet (C34557; Invitrogen) at a final concentration of 1:1,250 in PBS before culture. These cells were harvested after 3 d of incubation and analyzed by flow cytometry. For the cytokine production assays, cells were co-cultured overnight, then harvested and stimulated by PMA (2 ng/ml, P8139; Sigma-Aldrich) and ionomycin (10 ng/ml, I0634; Sigma-Aldrich). GolgiStop (1 µl/ml, 554724; BD Biosciences) was added to the media, and cells were then incubated overnight and analyzed by flow cytometry the next day.

RNA-seq

For RNA-seq, $TCRb^{low}$ $CD69^-CD44^-$ and $TCRb^{low}$ $CD69^+CD44^-$ DP thymocytes from control *Lsd1*$^{fl/fl}$ and *hCD2-iCre;Lsd1*$^{fl/fl}$ mice were sorted using a FACSAria flow cytometer (BD Biosciences). Total RNA was extracted using the Arcturus PicoPure RNA Isolation Kit (12204-01; Applied Biosystems). RNA-seq libraries were constructed using the TruSeq Stranded mRNA LT Sample Prep Kit (RS-122-2101; Illumina) with polyadenylic acid purification. Each sample used 1 µg total RNA input. The libraries were sequenced using HiSeq 2500 Rapid Run with 2 × 100 bp sequencing. RNA-seq was performed by the NICHD Molecular Genomics Core.

Four biological replicates and two technical replicates were sequenced for each RNA sample, yielding 28 million to 62 million paired-end reads of 101 bp. Reads were trimmed for low-quality bases from the 5′ end (minimum quality, 20) using cutadapt version 2.4 (Martin, 2011). Raw RNA-seq reads were aligned using HISAT2 version 2.1.0 (Kim et al., 2019), and reads were quantified with featureCounts version 1.6.4 (Liao et al., 2014). Differential expression analysis was performed using DESeq2 (Love et al., 2014). We used an FDR of <5% and a minimum FC of twofold to define statistical significance.

ChIP-seq

Whole thymi were dissected and processed, and thymocytes were fixed with 1% formaldehyde. Fixation was quenched with 0.125 M glycine. Thymocytes were lysed using a lysis buffer containing 5 mM Pipes (pH 8), 85 mM KCl, and 10 µl/ml Igepal and protease inhibitor. Lysates were then homogenized, and the nuclei were lysed using a nuclear lysis buffer containing 10 mM Tris-HCl (pH 8), 10 mM EDTA (pH 8), 1% SDS (vol/vol), and 10 µl/ml protease inhibitor. Isolated chromatin was sonicated to 200–500-bp fragments (Bioruptor; Diagenode). Sonicated DNA was then incubated with Protein A beads (Dynabeads; Invitrogen) conjugated to H3K4Me3 (MC315; MilliporeSigma), H3K4Me2 (AW30; MilliporeSigma), or H3K4Me1 (ab8895; Abcam) antibodies. Immunoprecipitated DNA fragments were isolated using a Takara DNA isolation kit. DNA libraries were prepared using a DNA SMART ChIP-Seq Kit (Takara), then sequenced using an Illumina HiSeq 2500 system with single-read rapid run kit (1 × 50 bp). ChIP-seq was performed by the NICHD Molecular Genomics Core. Two or three biological replicates

from WT and Lsd1-KO cells were sequenced for each ChIP-seq sample (H3K4me1, n = 2; H3K4me2, n = 2; H3K4me3, n = 3), yielding a total of 15 million to 25 million single-end reads of 51 bp. Each histone mark was sequenced in an independent run, along with two biological replicates of input DNA from WT and Lsd1-KO samples. Raw ChIP-seq reads were trimmed for low-quality bases as above, using cutadapt version 2.1 and aligned using bowtie2 version 2.3.4.3 (Langmead and Salzberg, 2012). Redundant reads were removed, and peak calling was performed using SICER version 1.1 (Zang et al., 2009). Differential binding analysis comparing Lsd1-KO with WT was performed using DiffBind version 2.10.0 with the DESeq2 analysis model using P value <0.01 to define statistical significance (Stark and Brown, 2011). The scatterplots comparing logarithmic FCs are colored on the basis of statistical significance in the CD69-KO versus WT comparison.

scRNA-seq

For cell sorting, total thymocytes from control *Lsd1*$^{fl/fl}$ and *hCD2-iCre;Lsd1*$^{fl/fl}$ mice were stained with fluorochrome-conjugated antibodies against CD4, CD8a, CD103, CD5, and CD69. Sorted populations were CD8 ISP: CD8$^+$ CD103$^-$ CD69$^-$ CD5^{lo}; DN: CD4$^-$ CD8$^-$; unsignaled DP: CD4$^+$ CD8$^+$ CD69$^{lo/-}$. A mixture of 5–10 × 10^3 cells comprising sorted DN, DP, and CD8 ISP thymocytes (ratio of ∼2:1:1) was loaded, separately for each genotype, on the 10X Chromium controller. Each library was constructed using the Next GEM Single Cell 5′ Reagent Kit (version 1.1) according to the manufacturer's instructions. Two biological replicates, each with two captures (one for each genotype), were processed separately. Libraries for each replicate pair were sequenced on one NextSeq run using 26 × 98 bp. Sequencing files were processed and mapped to mm10, and count matrices were extracted using the Cell Ranger single-cell software (version 5.0). Further analyses were performed in R using the Seurat package (version 4.0.3; Butler et al., 2018; Stuart et al., 2019). Each sample was preprocessed in Seurat by removing cells that were outliers for feature (gene) counts per cell (<500 or >10,000) or >5% mitochondrial genes per cell. To identify and exclude doublet cells, we used the DoubletFinder tool (McGinnis et al., 2019). The datasets were merged and integrated using reciprocal PCA with Seurat. Following normalization, UMAP dimensional reduction was performed using the first 30 principal components. Nearest neighbors were calculated using the first 30 dimensions, and clustering was performed with a resolution of 0.3; clusters comprising <1% of total cells were removed from further analysis. The *FindAllMarkers* function was used to identify cluster marker genes with a minimum $\log_2$FC threshold of +0.5 (cluster of interest over all other clusters). The *AddModuleScore* function was used to score each individual cell for indicated gene signatures. Violin plots for signature scores were constructed in GraphPad Prism software, and one-way ANOVA followed by Šidák's multiple comparisons test was used to calculate significance.

OP9-DL1 culture

For differentiation assays, 500 ETPs + DN2 cells or 10,000 DN3 cells were placed in 24-well plates and cultured in differentiation medium (α-MEM supplemented with 20% FBS, penicillin, streptomycin, and cytokines stem cell factor (30 ng/ml), IL-7 (30 ng/ml), Flt3 (30 ng/ml), GM-CSF (10 ng/ml), IL-3 (10 ng/ml), IL-6 (10 ng/ml), M-CSF (10 ng/ml), and G-CSF (10 ng/ml) on irradiated OP9-DL1 stromal cells, as described previously (Yang et al., 2015). Cytokines were purchased from PeproTech. ETP + DN2 and DN3 cells were differentiated for 7 d. Medium was refreshed with cytokines at day 4. For differentiation assays with LSD1 inhibitor (GSK-LSD1; Sigma-Aldrich), 500 ETP + DN2 and 10,000 DN3 cells were placed in 24-well plates and cultured in differentiation medium supplemented with LSD1 inhibitor added at 0.1 µM, 0.5 µM, 2.5 µM, or 12.5 µM on irradiated OP9-DL1 stromal cells for 7 d. Medium was refreshed with cytokines and inhibitor at day 4.

Online supplemental material

Fig. S1 shows FACS staining of DN thymocytes and Treg cells from *CD2-iCre;Lsd1*$^{fl/fl}$ mice and the phenotype of *CD4Cre;Lsd1*$^{fl/fl}$ mice. Fig. S2 shows additional analysis of RNA-seq data and cell cycle analysis of *CD2-iCre;Lsd1*$^{fl/fl}$ thymocytes. Fig. S3 shows a heatmap of IFN response genes in control and *CD2-iCre;Lsd1*$^{fl/fl}$ DP thymocytes and examples of alternate lineage genes that are mis-/overexpressed in *CD2-iCre;Lsd1*$^{fl/fl}$ DP thymocytes. Fig. S4 shows the gating strategy for cells collected for scRNA-seq, UMAP plots of replicate scRNA-seq experiments, and examples of genes differentially decorated by H3K4me1, H3K4me2, and H3K4me3 in *CD2-iCre;Lsd1*$^{fl/fl}$ thymocytes. Fig. S5 shows examples of genes strongly down-regulated in DP thymocytes that are nevertheless decorated with H3K4me3 in both control and *CD2-iCre;Lsd1*$^{fl/fl}$ thymocytes. Data S1 lists gene signatures used for scRNA-seq analysis. Data S2 lists RNA-seq data. Data S3 lists scRNA-seq metrics.

Data availability

RNA-seq, scRNA-seq, and ChIP-seq data are available in the Gene Expression Omnibus database (accession no. GSE156198). All unique/stable reagents generated in this study are available from the corresponding author with a completed Materials Transfer Agreement.

Acknowledgments

We thank M. Rosenfeld (University of California, San Diego, San Diego, CA) for providing the *Lsd1*$^{fl/fl}$ mice and Todd Macfarlan for helpful discussions. RNA-seq and ChIP-seq were performed by the NICHD Molecular Genomics Core and scRNA-seq was performed by the National Cancer Institute Sequencing Facility.

This work was supported by the intramural research program of the Eunice Kennedy Shriver NICHD (project 1ZIAHD001803) to P.E. Love.

Author contributions: D.B. Stamos, L.M. Clubb, L.B. Chopp, J. Nie, A. Das, Y. Ding, H. Venkataganesh, J. Lee, and D. El-Khoury performed experiments for the present study. A. Mitra provided bioinformatics support. L. Li, R. Bosselut, A. Bhandoola, and P.E. Love designed experiments and edited the manuscript. P.E. Love wrote the paper.

Disclosures: The authors declare no competing interests exist.

Submitted: 17 September 2020
Revised: 27 August 2021
Accepted: 30 September 2021

References

Albu, D.I., J. VanValkenburgh, N. Morin, D. Califano, N.A. Jenkins, N.G. Copeland, P. Liu, and D. Avram. 2011. Transcription factor Bcl11b controls selection of invariant natural killer T-cells by regulating glycolipid presentation in double-positive thymocytes. *Proc. Natl. Acad. Sci. USA.* 108:6211–6216. https://doi.org/10.1073/pnas.1014304108

Bernstein, B.E., T.S. Mikkelsen, X. Xie, M. Kamal, D.J. Huebert, J. Cuff, B. Fry, A. Meissner, M. Wernig, K. Plath, et al. 2006. A bivalent chromatin structure marks key developmental genes in embryonic stem cells. *Cell.* 125:315–326. https://doi.org/10.1016/j.cell.2006.02.041

Butler, A., P. Hoffman, P. Smibert, E. Papalexi, and R. Satija. 2018. Integrating single-cell transcriptomic data across different conditions, technologies, and species. *Nat. Biotechnol.* 36:411–420. https://doi.org/10.1038/nbt.4096

Chambers, S.M., N.C. Boles, K.Y. Lin, M.P. Tierney, T.V. Bowman, S.B. Bradfute, A.J. Chen, A.A. Merchant, O. Sirin, D.C. Weksberg, et al. 2007. Hematopoietic fingerprints: an expression database of stem cells and their progeny. *Cell Stem Cell.* 1:578–591. https://doi.org/10.1016/j.stem.2007.10.003

Chopp, L.B., V. Gopalan, T. Ciucci, A. Ruchinskas, Z. Rae, M. Lagarde, Y. Gao, C. Li, M. Bosticardo, F. Pala, et al. 2020. An integrated epigenomic and transcriptomic map of mouse and human αβ T cell development. *Immunity.* 53:1182–1201.e8. https://doi.org/10.1016/j.immuni.2020.10.024

Ciofani, M., and J.C. Zúñiga-Pflücker. 2010. Determining γδ versus αß T cell development. *Nat. Rev. Immunol.* 10:657–663. https://doi.org/10.1038/nri2820

Doan, L.L., S.D. Porter, Z. Duan, M.M. Flubacher, D. Montoya, P.N. Tsichlis, M. Horwitz, C.B. Gilks, and H.L. Grimes. 2004. Targeted transcriptional repression of Gfi1 by GFI1 and GFI1B in lymphoid cells. *Nucleic Acids Res.* 32:2508–2519. https://doi.org/10.1093/nar/gkh570

Fraszczak, J., and T. Möröy. 2021. The transcription factors GFI1 and GFI1B as modulators of the innate and acquired immune response. *Adv. Immunol.* 149:35–94. https://doi.org/10.1016/bs.ai.2021.03.003

Gioulbasani, M., A. Galaras, S. Grammenoudi, P. Moulos, A.L. Dent, M. Sigvardsson, P. Hatzis, B.L. Kee, and M. Verykokakis. 2020. The transcription factor BCL-6 controls early development of innate-like T cells. *Nat. Immunol.* 21:1058–1069. https://doi.org/10.1038/s41590-020-0737-y

Hatano, S., T. Murakami, N. Noguchi, H. Yamada, and Y. Yoshikai. 2017. $CD5^-$ $NK1.1^+$ γδ T cells that develop in a Bcl11b-independent manner participate in early protection against infection. *Cell Rep.* 21:1191–1202. https://doi.org/10.1016/j.celrep.2017.10.007

Hatzi, K., H. Geng, A.S. Doane, C. Meydan, R. LaRiviere, M. Cardenas, C. Duy, H. Shen, M.N.C. Vidal, T. Baslan, et al. 2019. Histone demethylase LSD1 is required for germinal center formation and BCL6-driven lymphomagenesis. *Nat. Immunol.* 20:86–96. https://doi.org/10.1038/s41590-018-0273-1

Hayes, S.M., and P.E. Love. 2007. A retrospective on the requirements for gammadelta T-cell development. *Immunol. Rev.* 215:8–14. https://doi.org/10.1111/j.1600-065X.2006.00476.x

Hirose, S., M. Touma, R. Go, Y. Katsuragi, Y. Sakuraba, Y. Gondo, M. Abe, K. Sakimura, Y. Mishima, and R. Kominami. 2015. Bcl11b prevents the intrathymic development of innate CD8 T cells in a cell intrinsic manner. *Int. Immunol.* 27:205–215. https://doi.org/10.1093/intimm/dxu104

Hosokawa, H., M. Romero-Wolf, M.A. Yui, J. Ungerbäck, M.L.G. Quiloan, M. Matsumoto, K.I. Nakayama, T. Tanaka, and E.V. Rothenberg. 2018. Bcl11b sets pro-T cell fate by site-specific cofactor recruitment and by repressing Id2 and Zbtb16. *Nat. Immunol.* 19:1427–1440. https://doi.org/10.1038/s41590-018-0238-4

Hosseini, A., and S. Minucci. 2017. A comprehensive review of lysine-specific demethylase 1 and its roles in cancer. *Epigenomics.* 9:1123–1142. https://doi.org/10.2217/epi-2017-0022

Huang, J., R. Sengupta, A.B. Espejo, M.G. Lee, J.A. Dorsey, M. Richter, S. Opravil, R. Shiekhattar, M.T. Bedford, T. Jenuwein, and S.L. Berger. 2007. p53 is regulated by the lysine demethylase LSD1. *Nature.* 449:105–108. https://doi.org/10.1038/nature06092

Ivanova, N.B., J.T. Dimos, C. Schaniel, J.A. Hackney, K.A. Moore, and I.R. Lemischka. 2002. A stem cell molecular signature. *Science.* 298:601–604. https://doi.org/10.1126/science.1073823

Kastner, P., S. Chan, W.K. Vogel, L.J. Zhang, A. Topark-Ngarm, O. Golonzhka, B. Jost, S. Le Gras, M.K. Gross, and M. Leid. 2010. Bcl11b represses a mature T-cell gene expression program in immature $CD4^{(+)}CD8^{(+)}$ thymocytes. *Eur. J. Immunol.* 40:2143–2154. https://doi.org/10.1002/eji.200940258

Kerenyi, M.A., Z. Shao, Y.J. Hsu, G. Guo, S. Luc, K. O'Brien, Y. Fujiwara, C. Peng, M. Nguyen, and S.H. Orkin. 2013. Histone demethylase Lsd1 represses hematopoietic stem and progenitor cell signatures during blood cell maturation. *eLife.* 2:e00633. https://doi.org/10.7554/eLife.00633

Kim, D., J.M. Paggi, C. Park, C. Bennett, and S.L. Salzberg. 2019. Graph-based genome alignment and genotyping with HISAT2 and HISAT-genotype. *Nat. Biotechnol.* 37:907–915. https://doi.org/10.1038/s41587-019-0201-4

Krivtsov, A.V., D. Twomey, Z. Feng, M.C. Stubbs, Y. Wang, J. Faber, J.E. Levine, J. Wang, W.C. Hahn, D.G. Gilliland, et al. 2006. Transformation from committed progenitor to leukaemia stem cell initiated by MLL-AF9. *Nature.* 442:818–822. https://doi.org/10.1038/nature04980

Langmead, B., and S.L. Salzberg. 2012. Fast gapped-read alignment with Bowtie 2. *Nat. Methods.* 9:357–359. https://doi.org/10.1038/nmeth.1923

Le Douce, V., L. Colin, L. Redel, T. Cherrier, G. Herbein, D. Aunis, O. Rohr, C. Van Lint, and C. Schwartz. 2012. LSD1 cooperates with CTIP2 to promote HIV-1 transcriptional silencing. *Nucleic Acids Res.* 40:1904–1915. https://doi.org/10.1093/nar/gkr857

Li, H., M. Ji, K.D. Klarmann, and J.R. Keller. 2010. Repression of Id2 expression by Gfi-1 is required for B-cell and myeloid development. *Blood.* 116:1060–1069. https://doi.org/10.1182/blood-2009-11-255075

Li, Q., J. Zou, M. Wang, X. Ding, I. Chepelev, X. Zhou, W. Zhao, G. Wei, J. Cui, K. Zhao, et al. 2014. Critical role of histone demethylase Jmjd3 in the regulation of $CD4^+$ T-cell differentiation. *Nat. Commun.* 5:5780. https://doi.org/10.1038/ncomms6780

Liao, Y., G.K. Smyth, and W. Shi. 2014. featureCounts: an efficient general purpose program for assigning sequence reads to genomic features. *Bioinformatics.* 30:923–930. https://doi.org/10.1093/bioinformatics/btt656

Liu, P., P. Li, and S. Burke. 2010. Critical roles of Bcl11b in T-cell development and maintenance of T-cell identity. *Immunol. Rev.* 238:138–149. https://doi.org/10.1111/j.1600-065X.2010.00953.x

Love, M.I., W. Huber, and S. Anders. 2014. Moderated estimation of fold change and dispersion for RNA-seq data with DESeq2. *Genome Biol.* 15:550. https://doi.org/10.1186/s13059-014-0550-8

Manna, S., J.K. Kim, C. Baugé, M. Cam, Y. Zhao, J. Shetty, M.S. Vacchio, E. Castro, B. Tran, L. Tessarollo, and R. Bosselut. 2015. Histone H3 Lysine 27 demethylases Jmjd3 and Utx are required for T-cell differentiation. *Nat. Commun.* 6:8152. https://doi.org/10.1038/ncomms9152

Martin, M. 2011. Cutadapt removes adapter sequences from high-throughput sequencing reads. *EMBnet. J.* 17:10–12. https://doi.org/10.14806/ej.17.1.200

Mingueneau, M., T. Kreslavsky, D. Gray, T. Heng, R. Cruse, J. Ericson, S. Bendall, M.H. Spitzer, G.P. Nolan, K. Kobayashi, et al. Immunological Genome Consortium. 2013. The transcriptional landscape of αβ T cell differentiation. *Nat. Immunol.* 14:619–632. https://doi.org/10.1038/ni.2590

Miyazaki, M., K. Miyazaki, M. Itoi, Y. Katoh, Y. Guo, R. Kanno, Y. Katoh-Fukui, H. Honda, T. Amagai, M. van Lohuizen, et al. 2008. Thymocyte proliferation induced by pre-T cell receptor signaling is maintained through polycomb gene product Bmi-1-mediated Cdkn2a repression. *Immunity.* 28:231–245. https://doi.org/10.1016/j.immuni.2007.12.013

Perillo, B., A. Tramontano, A. Pezone, and A. Migliaccio. 2020. LSD1: more than demethylation of histone lysine residues. *Exp. Mol. Med.* 52:1936–1947. https://doi.org/10.1038/s12276-020-00542-2

Rothenberg, E.V., and J.A. Zhang. 2012. T-cell identity and epigenetic memory. *Curr. Top. Microbiol. Immunol.* 356:117–143.

Rothenberg, E.V., H.Y. Kueh, M.A. Yui, and J.A. Zhang. 2016. Hematopoiesis and T-cell specification as a model developmental system. *Immunol. Rev.* 271:72–97. https://doi.org/10.1111/imr.12417

Saleque, S., J. Kim, H.M. Rooke, and S.H. Orkin. 2007. Epigenetic regulation of hematopoietic differentiation by Gfi-1 and Gfi-1b is mediated by the cofactors CoREST and LSD1. *Mol. Cell.* 27:562–572. https://doi.org/10.1016/j.molcel.2007.06.039

Shah, D.K., and J.C. Zúñiga-Pflücker. 2014. An overview of the intrathymic intricacies of T cell development. *J. Immunol.* 192:4017–4023. https://doi.org/10.4049/jimmunol.1302259

Sheng, W., M.W. LaFleur, T.H. Nguyen, S. Chen, A. Chakravarthy, J.R. Conway, Y. Li, H. Chen, H. Yang, P.H. Hsu, et al. 2018. LSD1 ablation stimulates anti-tumor immunity and enables checkpoint blockade. *Cell.* 174:549–563.e19. https://doi.org/10.1016/j.cell.2018.05.052

Shi, L.Z., J. Saravia, H. Zeng, N.S. Kalupahana, C.S. Guy, G. Neale, and H. Chi. 2017. Gfi1-Foxo1 axis controls the fidelity of effector gene expression and developmental maturation of thymocytes. *Proc. Natl. Acad. Sci. USA.* 114:E67–E74. https://doi.org/10.1073/pnas.1617669114

Solanki, A., D.C. Yánez, C.I. Lau, J. Rowell, A. Barbarulo, S. Ross, H. Sahni, and T. Crompton. 2020. The transcriptional repressor Bcl6 promotes pre-

TCR-induced thymocyte differentiation and attenuates Notch1 activation. *Development.* 147:dev192203. https://doi.org/10.1242/dev.192203

Sprüssel, A., J.H. Schulte, S. Weber, M. Necke, K. Händschke, T. Thor, K.W. Pajtler, A. Schramm, K. König, L. Diehl, et al. 2012. Lysine-specific demethylase 1 restricts hematopoietic progenitor proliferation and is essential for terminal differentiation. *Leukemia.* 26:2039–2051. https://doi.org/10.1038/leu.2012.157

Stark, R., and G. Brown. 2011. DiffBind: Differential binding analysis of ChIP-Seq peak data. http://bioconductor.org/packages/release/bioc/vignettes/DiffBind/inst/doc/DiffBind.pdf (accessed April 4, 2019)

Stuart, T., A. Butler, P. Hoffman, C. Hafemeister, E. Papalexi, W.M. Mauck III, Y. Hao, M. Stoeckius, P. Smibert, and R. Satija. 2019. Comprehensive integration of single-cell data. *Cell.* 177:1888–1902.e21. https://doi.org/10.1016/j.cell.2019.05.031

Tanaka, H., T. Naito, S. Muroi, W. Seo, R. Chihara, C. Miyamoto, R. Kominami, and I. Taniuchi. 2013. Epigenetic Thpok silencing limits the time window to choose CD4(+) helper-lineage fate in the thymus. *EMBO J.* 32:1183–1194. https://doi.org/10.1038/emboj.2013.47

McGinnis, C.S., D.M. Patterson, J. Winkler, D.N. Conrad, M.Y. Hein, V. Srivastava, J.L. Hu, L.M. Murrow, J.S. Weissman, Z. Werb, et al. 2019. MULTI-seq: sample multiplexing for single-cell RNA sequencing using lipid-tagged indices. *Nat. Methods.* 16:619–626. https://doi.org/10.1038/s41592-019-0433-8

van der Meer, L.T., J.H. Jansen, and B.A. van der Reijden. 2010. Gfi1 and Gfi1b: key regulators of hematopoiesis. *Leukemia.* 24:1834–1843. https://doi.org/10.1038/leu.2010.195

Vastenhouw, N.L., and A.F. Schier. 2012. Bivalent histone modifications in early embryogenesis. *Curr. Opin. Cell Biol.* 24:374–386. https://doi.org/10.1016/j.ceb.2012.03.009

Voehringer, D., H.E. Liang, and R.M. Locksley. 2008. Homeostasis and effector function of lymphopenia-induced "memory-like" T cells in constitutively T cell-depleted mice. *J. Immunol.* 180:4742–4753. https://doi.org/10.4049/jimmunol.180.7.4742

Wakabayashi, Y., H. Watanabe, J. Inoue, N. Takeda, J. Sakata, Y. Mishima, J. Hitomi, T. Yamamoto, M. Utsuyama, O. Niwa, et al. 2003. Bcl11b is required for differentiation and survival of alphabeta T lymphocytes. *Nat. Immunol.* 4:533–539. https://doi.org/10.1038/ni927

Wang, J., K. Scully, X. Zhu, L. Cai, J. Zhang, G.G. Prefontaine, A. Krones, K.A. Ohgi, P. Zhu, I. Garcia-Bassets, et al. 2007. Opposing LSD1 complexes function in developmental gene activation and repression programmes. *Nature.* 446:882–887. https://doi.org/10.1038/nature05671

Wells, A.D., and P.A. Morawski. 2014. New roles for cyclin-dependent kinases in T cell biology: linking cell division and differentiation. *Nat. Rev. Immunol.* 14:261–270. https://doi.org/10.1038/nri3625

Whyte, W.A., S. Bilodeau, D.A. Orlando, H.A. Hoke, G.M. Frampton, C.T. Foster, S.M. Cowley, and R.A. Young. 2012. Enhancer decommissioning by LSD1 during embryonic stem cell differentiation. *Nature.* 482:221–225. https://doi.org/10.1038/nature10805

Yang, Q., F. Li, C. Harly, S. Xing, L. Ye, X. Xia, H. Wang, X. Wang, S. Yu, X. Zhou, et al. 2015. TCF-1 upregulation identifies early innate lymphoid progenitors in the bone marrow. *Nat. Immunol.* 16:1044–1050. https://doi.org/10.1038/ni.3248

Yücel, R., H. Karsunky, L. Klein-Hitpass, and T. Möröy. 2003. The transcriptional repressor Gfi1 affects development of early, uncommitted c-Kit+ T cell progenitors and CD4/CD8 lineage decision in the thymus. *J. Exp. Med.* 197:831–844. https://doi.org/10.1084/jem.20021417

Yui, M.A., N. Feng, and E.V. Rothenberg. 2010. Fine-scale staging of T cell lineage commitment in adult mouse thymus. *J. Immunol.* 185:284–293. https://doi.org/10.4049/jimmunol.1000679

Zang, C., D.E. Schones, C. Zeng, K. Cui, K. Zhao, and W. Peng. 2009. A clustering approach for identification of enriched domains from histone modification ChIP-Seq data. *Bioinformatics.* 25:1952–1958. https://doi.org/10.1093/bioinformatics/btp340

Zhang, J.A., A. Mortazavi, B.A. Williams, B.J. Wold, and E.V. Rothenberg. 2012. Dynamic transformations of genome-wide epigenetic marking and transcriptional control establish T cell identity. *Cell.* 149:467–482. https://doi.org/10.1016/j.cell.2012.01.056

Supplemental material

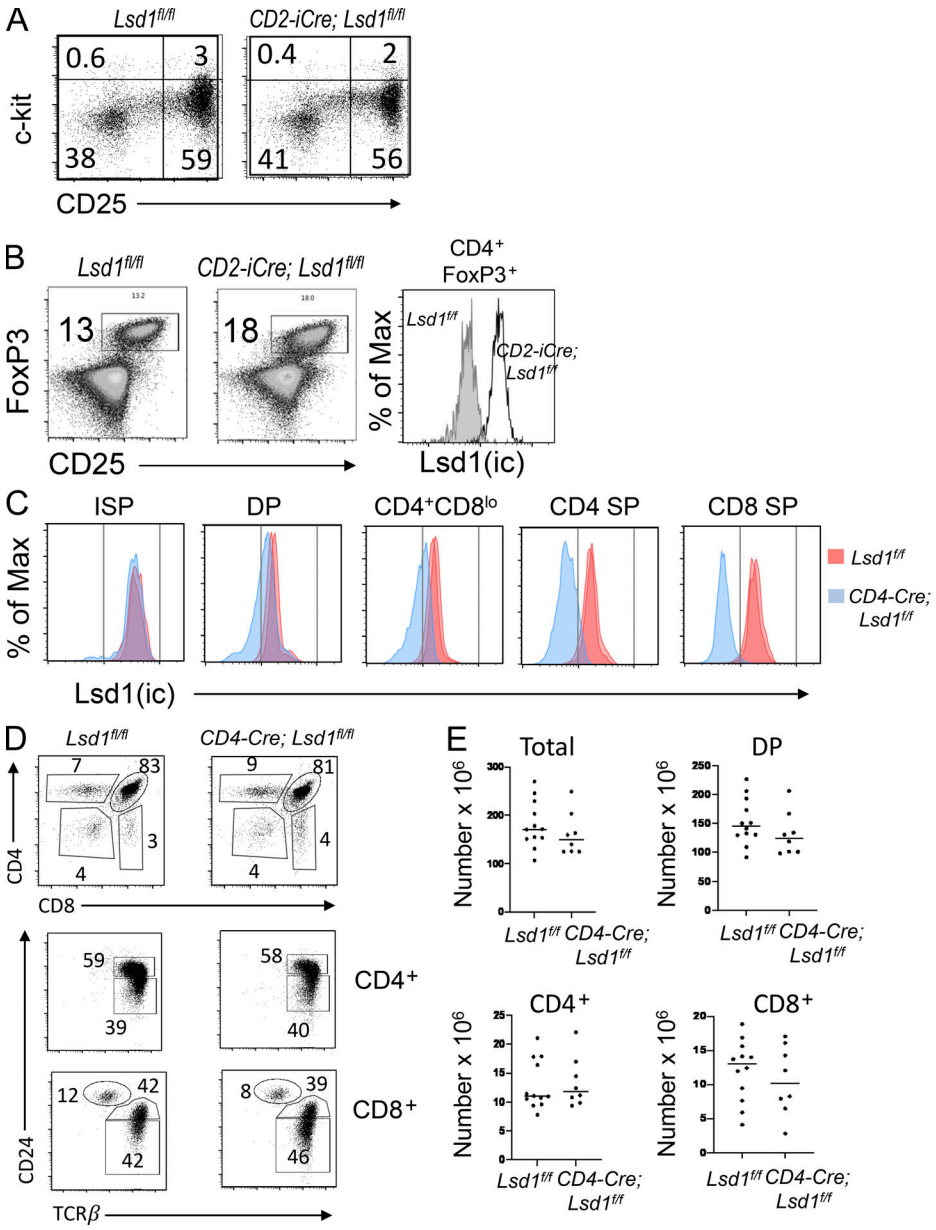

Figure S1. **DN and Treg phenotype of *CD2-iCre;Lsd1*$^{fl/fl}$ mice and phenotype of *CD4-Cre;Lsd1*$^{fl/fl}$ mice. (A)** c-Kit versus CD25 surface staining of lineage-negative (DN) thymocytes from *Lsd1*$^{fl/fl}$ and *CD2-iCre;Lsd1*$^{fl/fl}$ mice. Quadrants starting clockwise from upper left: DN1, DN2, DN3, and DN4. One representative of four experiments is shown. **(B)** Left: FoxP3 intracellular (ic) staining versus CD25 surface staining profiles of gated CD4$^+$ spleen T cells from *Lsd1*$^{fl/fl}$ and *CD2-iCre;Lsd1*$^{fl/fl}$ mice. Right: Intracellular staining for Lsd1 in gated CD4$^+$ FoxP3$^+$ T cells from *Lsd1*$^{fl/fl}$ and *CD2-iCre;Lsd1*$^{fl/fl}$ mice. **(C)** Intracellular staining for Lsd1 in thymocytes from *Lsd1*$^{fl/fl}$ and *CD4-Cre;Lsd1*$^{fl/fl}$ mice. Lsd1 staining is shown in cells within gated thymocyte subpopulations. **(D)** Phenotype of *CD4-Cre;Lsd1*$^{fl/fl}$ mice. Top: CD4 versus CD8 surface staining profiles of total thymocytes from *Lsd1*$^{fl/fl}$ and *CD4-Cre;Lsd1*$^{fl/fl}$ mice. Numbers in each gate are the percentages of total cells. Bottom: CD24 versus TCRβ staining profiles of gated CD4 SP and CD8 SP thymocytes showing absence of a maturational defect in thymocytes from *CD4-Cre;Lsd1*$^{fl/fl}$ mice. **(E)** Numbers of total, DP, CD4 SP, and CD8 SP thymocytes from *Lsd1*$^{fl/fl}$ and *CD4-Cre;Lsd1*$^{fl/fl}$ mice. Results shown in A–D are representative of three or more experiments.

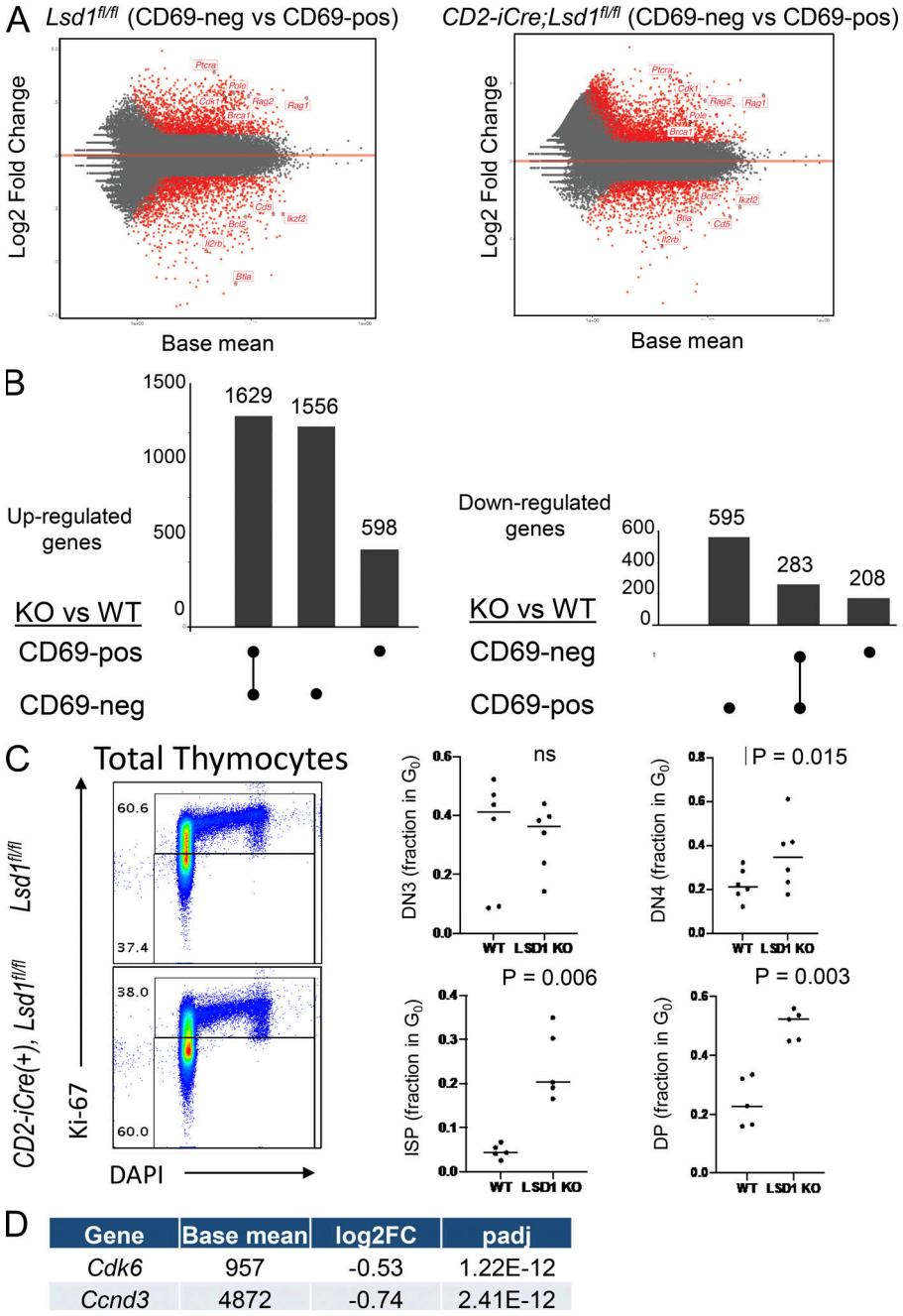

Gene	Base mean	log2FC	padj
Cdk6	957	-0.53	1.22E-12
Ccnd3	4872	-0.74	2.41E-12

Figure S2. **Dysregulated gene expression in *CD2-iCre;Lsd1$^{fl/fl}$* DP thymocytes and cell cycle analysis of *CD2-iCre;Lsd1$^{fl/fl}$* thymocytes. (A)** MA plots comparing gene expression in CD69^{-} versus CD69^{+} thymocytes from *Lsd1$^{fl/fl}$* mice (left) or *CD2-iCre;Lsd1$^{fl/fl}$* mice (right). Red dots indicate genes that are significantly changed in KO versus WT thymocytes. **(B)** Upset plots showing the number of unique overexpressed genes (left) or down-regulated genes (right) in *CD2-iCre;Lsd1$^{fl/fl}$* DP thymocytes versus *Lsd1$^{fl/fl}$* DP thymocytes. Note that the number of up-regulated genes is much greater than down-regulated genes in both CD69^{+} and CD69^{-} *CD2-iCre;Lsd1$^{fl/fl}$* DP thymocytes. **(C)** Left: Cell cycle analysis by Ki-67 versus DAPI staining of total thymocytes from *Lsd1$^{fl/fl}$* and *CD2-iCre;Lsd1$^{fl/fl}$* mice reveals an increase in G_0 phase cells from *CD2-iCre;Lsd1$^{fl/fl}$* mice. Right: Cell cycle analysis of thymocyte subsets confirms the increase in G_0 phase DN4, ISP, and DP cells from *CD2-iCre;Lsd1$^{fl/fl}$* mice. **(D)** *Cdk6* and *Ccnd3* are down-regulated (negative $\log_2$FC) in Lsd1 KO CD69^{-} DP thymocytes.

A

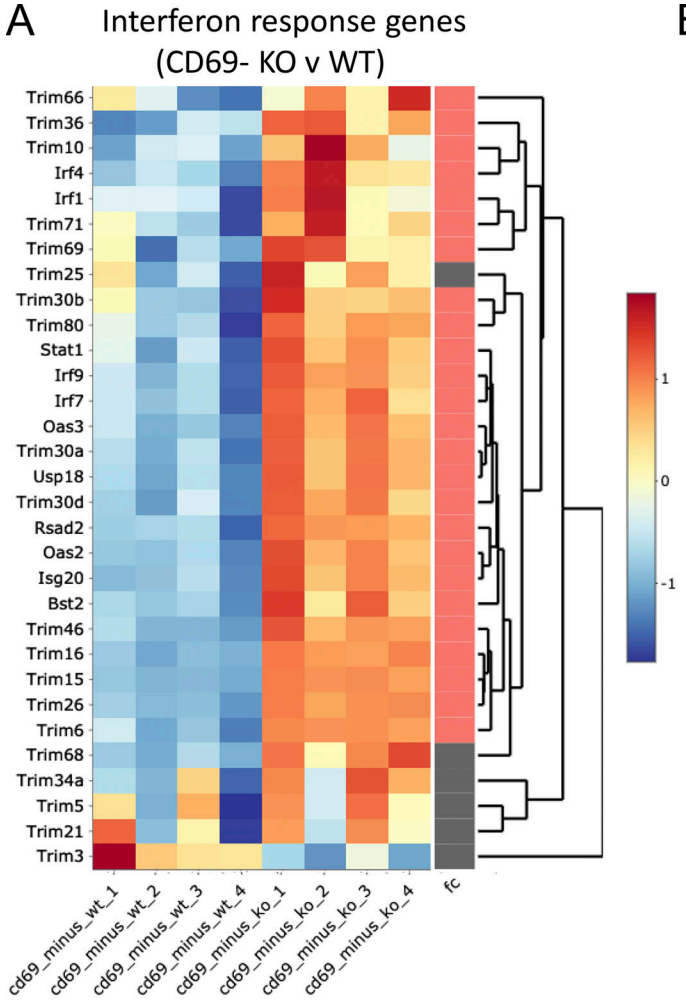

B

gene	baseMean	log2FC	padj
Cebpb			
Nr1d1	99	2.8	1.69E-26
Dusp1	1463	1.9	1.99E-11
Bag3	24	1.2	1.76E-04
Fos	2145	3.6	1.66E-22
Serpini1	53	0.8	2.90E-05
Dbp	55	0.5	1.19E-03
PMID: 15985538			
Egr2			
Zbtb16	20	6.2	1.54E-15
Il2rb	63	3.7	2.42E-08
Id2	141	1.3	1.45E-08
Ccnd2	660	6.2	1.66E-67
Slc9a9	4638	1.2	1.97E-69
Ptprv	249	2.6	1.32E-79
PMID: 25123285; 22306690			
Zbtb16			
Rora	103	1.1	4.18E-05
Maf	1175	7.2	3.95E-270
Rarg	94	6.2	1.17E-74
Tsc22d1	684	1.2	3.39E-42
Bcl6	1655	-1.1	9.00E-29
Runx3	246	2.7	7.74E-174
Il18r1	1979	10.1	6.05E-248
PMID: 27325774			
Irf4			
Pim2	81	1.1	1.09E-10
Ifi27	390	1.9	4.97E-95
Ifi44	23	6.8	3.03E-16
Prdm1	30	1.5	6.99E-08
PMID: 25207815			

Figure S3. **Overexpression of IFN response genes and alternate lineage genes in *CD2-iCre;Lsd1$^{fl/fl}$* DP thymocytes. (A)** Heatmap of IFN response gene expression in CD69^{-} DP thymocytes from *Lsd1$^{fl/fl}$* and *CD2-iCre;Lsd1$^{fl/fl}$* mice. Red bars on the right indicate significantly changed genes. **(B)** Overexpression of Cebpb, Egr2, Zbtb16, and Irf4 target genes in *CD2-iCre;Lsd1$^{fl/fl}$* CD69^{-} DP thymocytes.

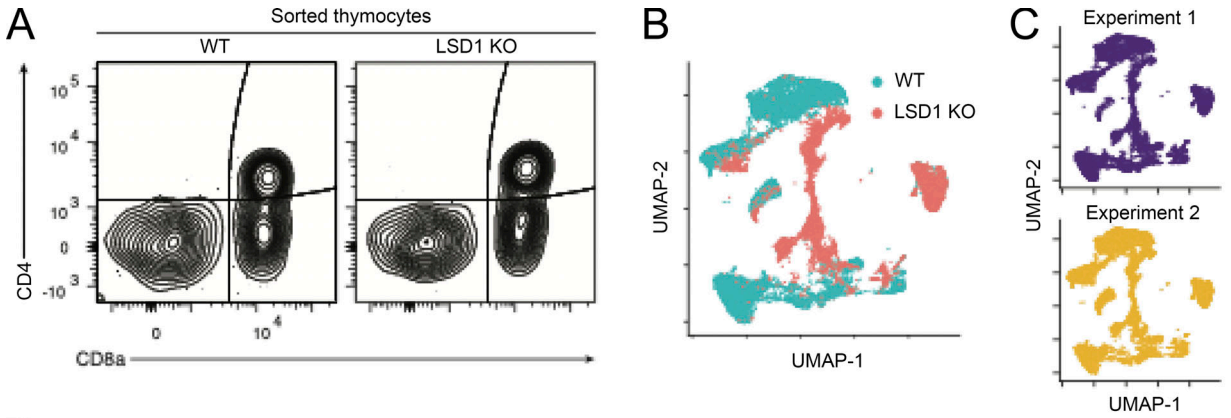

D

Gene	Base mean	log2FC	padj
Adora2a	145	0.99	2.91E-07
Tpd52	264	2.34	3.30E-245
Esm1	21	4.95	5.63E-27
Maf	1175	7.20	3.95E-270
Sell	1309	1.51	2.03E-75
Tjp2	143	4.43	1.26E-132

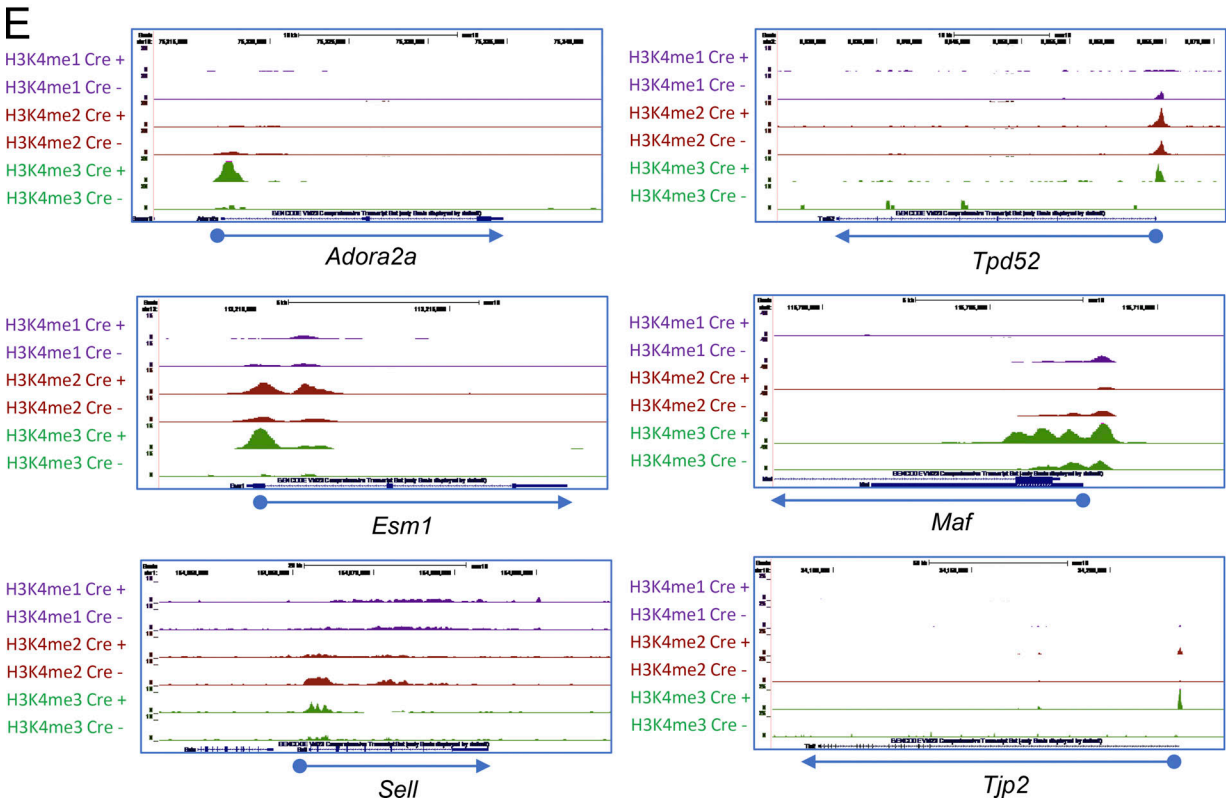

Figure S4. **scRNA-seq results of duplicate experiments and variable H3K4-me1,2,3 decoration of up-regulated genes in *CD2-iCre;Lsd1$^{fl/fl}$* DP thymocytes. (A)** FACS plot of sorted cells used for scRNA-seq. **(B)** Overlapped UMAP plots from *Lsd1$^{fl/fl}$* (WT) and *CD2-iCre;Lsd1$^{fl/fl}$* (LSD1 KO) thymocytes. **(C)** UMAP plots of *CD2-iCre;Lsd1$^{fl/fl}$* (LSD1 KO) and *Lsd1$^{fl/fl}$* (WT) thymocytes from biological replicate experiments. **(D and E)** Variable decoration with H3K4me1 and H3K4me2 at overexpressed genes in *CD2-iCre;Lsd1$^{fl/fl}$* DP thymocytes. **(D)** Sample of up-regulated genes in *CD2-iCre;Lsd1$^{fl/fl}$* CD69^{-} DP thymocytes. Positive $\log_2$FC values indicate that genes are overexpressed in KO thymocytes versus WT thymocytes. **(E)** UCSC Genome browser shots showing H3K4me1, H3K4me2, and H3K4me3 ChIP-seq plots for *Lsd1$^{fl/fl}$* and *CD2-iCre;Lsd1$^{fl/fl}$* CD69^{-} DP thymocytes near the indicated genes. Screenshots are one representative of three ChIP-seq replicates.

A

Gene	Basemean	log2FC	padj
Hoxa9	1.46	2.12	0.072
Tal1	<1	2.3	0.27
Gata2	1.24	-0.23	0.89
Lmo2	<1	2.75	0.017
Lyl1	3	0.84	0.021
Hhex	6	1.93	0.05

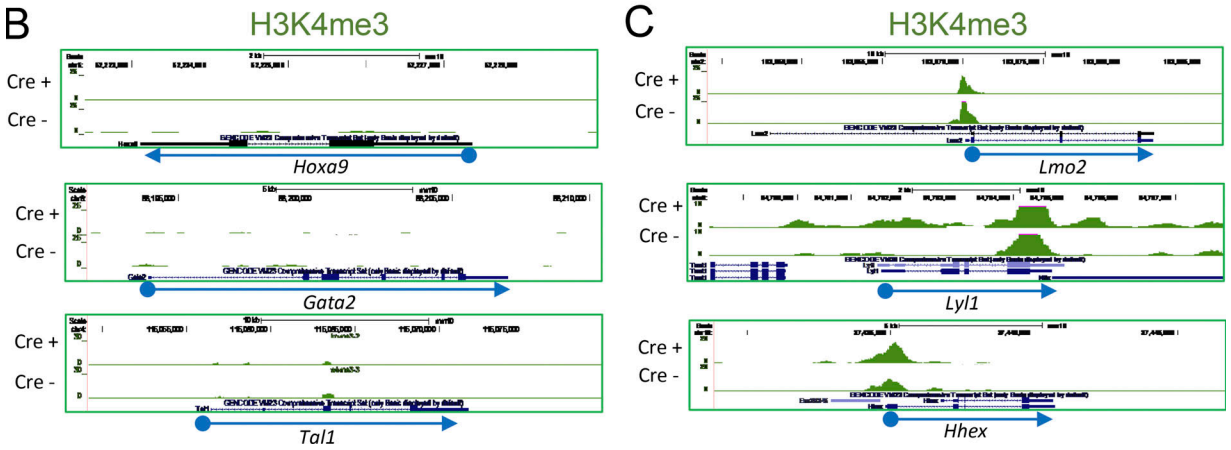

Figure S5. **H3K4 trimethylation is not sufficient for gene expression. (A)** Expression level of the indicated HSC-expressed genes in *CD2-iCre;Lsd1*$^{fl/fl}$ CD69^{-} DP thymocytes. **(B)** UCSC Genome Browser screenshots showing H3K4me3 ChIP-seq results at the promoters of *Hoxa9*, *Gata2*, and *Tal1*. **(C)** UCSC Genome Browser screenshots showing H3K4me3 ChIP-seq results at the promoters of *Lmo2*, *Lyl1*, and *Hhex*.

Data S1–S3 are provided online as separate Excel files. Data S1 lists gene signatures used for scRNA-seq analysis. Data S2 lists RNA-seq data. Data S3 lists scRNA-seq metrics.